1999) and UvrB from *Bacillus caldotenax* (Theis et al., 1999), which are members of the superfamily 2. These structural studies revealed that the helicase motifs constitute an NTPase activity site at the interface of two domains and that a cleft between these two domains and a third is a binding site for single-stranded nucleic acids, suggesting that the same mechanisms underlie NTP hydrolysis and strand unwinding. However, Borowski et al. have shown that the inhibitory effects of halogenated benzimidazole and benzotriazole derivatives against NTPase and the helicase activities of NS3 proteins varied among JEV, WNV and HCV, suggesting that the enzymatic active sites of these viruses are structurally different (Borowski et al., 2003).

In this study, we examined a refined three-dimensional structure of the JEV helicase/NTPase domain. The three-lobed structure displays an asymmetric distribution of charges on its surface and contains a tunnel large enough to accommodate single-stranded RNA. The overall structure is similar to other flavivirus helicases (Wu et al., 2005; Xu et al., 2005; Yao et al., 1997) and each of the motifs I, II and VI is composed of an NTP-binding pocket. Mutation analyses revealed that the residues in the Walker A motif and the motif VI were crucial for not only ATPase and helicase activities but also virus replication. The detailed structural comparison among members of the family *Flaviviridae* should provide further insight into the molecular mechanisms of viral RNA replication.

Results

Overall structure

The structure of the JEV helicase/NTPase domain (amino acid residues 171 to 619) was determined using the molecular replacement method based on data collected at 1.8 Å resolution. A summary of the data collection, phasing, density modification and structure refinement statistics is shown in Table 1. JEV NS3 helicase is composed of three domains of roughly equal size with DEN, YFV and HCV helicases (Fig. 1C). Like other helicases, each domain 1 or 2 of the JEV helicase forms an α/β domain with a RecA-like topology. The available structures suggest that nucleic acids bind across the interface of two RecA-like fold domains (Velankar et al., 1999). Domain 1 (amino acid residues 171–328) is composed of four α-helices and five β-sheets. The cluster of the β-strands is surrounded by three of the four α-helices. The seven sequence motifs of superfamily 2 helicases (Koonin, 1991) were assigned to domains 1 and 2 (Fig. 1A). Domain 1 has two ATP-binding motifs, Walker A (motif I; GSGKT) and Walker B (motif II; DEAH), which are conserved among three helicase superfamilies. Domain 2 (amino acid residues 329–482) is composed of three α-helices and eight β-strands and divided into two subunits. One subunit is surrounded by six β-strands and three α-helices, and the other has two β-strands penetrating into domain 3. The motifs Ia, II and V face each other across the domain boundary and participate in a tight configuration. An arginine finger in motif VI (QRRGRVGR) in domain 2 is thought to be crucial for NTP hydrolysis (Ahmadian et al., 1997; Caruthers and McKay, 2002; Niedenzu et al., 2001). Domain 3 (amino acid residues 483–619) is composed of seven α-helices and two β-strands.

Table 1
Data collection and refinement statistics

Diffraction data	
X-ray source	SPring-8 BL44-XU
Detector	Mac Science DIP6040
Temperature (K)	100
Space group	$P2_1$
Unit-cell parameters	
a (Å)	59.31
b (Å)	68.31
c (Å)	65.48
β (°)	116.89
X-ray wavelength (Å)	0.9000
Resolution range (Å)	50–1.80 (1.86–1.80)
Total reflections	83514 (8266)
Multiplicity	4.2 (4.2)
R_{merge} [a]	0.051 (0.434)
Completeness (%)	99.9 (99.5)
I/sigma I	20.8 (3.8)
Refinement statistics	
Resolution range (Å)	20–1.8
Unique reflections	42747 (4264)
R (%)	19.7
R_{free} (%)	24.7
RMSD bond length (Å)	0.016
RMSD bond angle (Å)	1.611
Water molecules (no.)	413

Values in square brackets refer to the highest resolution shell.
[a] $R_{merge} = \Sigma_{hkl}\Sigma_i|I(hkl)_i - \langle I(hkl)/\Sigma_{hkl}I(hkl)\rangle|$, where $I(hkl)_i$ is the *i*th measurement of the intensity of reflection *hkl* and $\langle I(hkl)\rangle$ is the mean intensity of reflection *hkl*.

NTP-binding region

To examine the ATP-binding state of the JEV helicase, a hypothetical ATP-binding model was built (Fig. 2). The model showed that an ATP molecule was localized with the cleft between domains 1 and 2 (Fig. 2A). In the ATP-binding pocket formed by the cleft, an ATP molecule was associated with the Walker A motif (motif I), Walker B motif (motif II), and motif VI (Fig. 2B). All residues in these motifs were well conserved among the DEAH-box helicase proteins (Schmid and Linder, 1992). Based on the crystal structure of JEV helicase, positively charged residues, Lys^{200}, Arg^{461} and Arg^{464} are present in the pocket of the active sites of motifs I, II and VI. Lys^{200} protrudes into the pocket, recognizes the β-or γ-phosphate of ATP and forms a salt bridge with Asp^{285} and Glu^{286} for stabilization of the active site structure. Arg^{461} and Arg^{464} in motif VI form an arginine finger, work as sensors recognizing the γ-and α-phosphate of ATP, and are critical for conformational switching upon ATP hydrolysis (Ahmadian et al., 1997; Caruthers and McKay, 2002; Niedenzu et al., 2001). One water is coordinated with residues Glu^{286}, His^{288} and Gln^{457} at distances of 2.73 Å, 2.67 Å and 4.0 Å, respectively. His^{288} is essential for RNA-unwinding activity (Utama et al., 2000a,b).

Nucleic acid-binding site

The domain 3 of JEV helicase interacts with domains 1 and 2 to form a groove at the domain boundary (Fig. 3). Among the

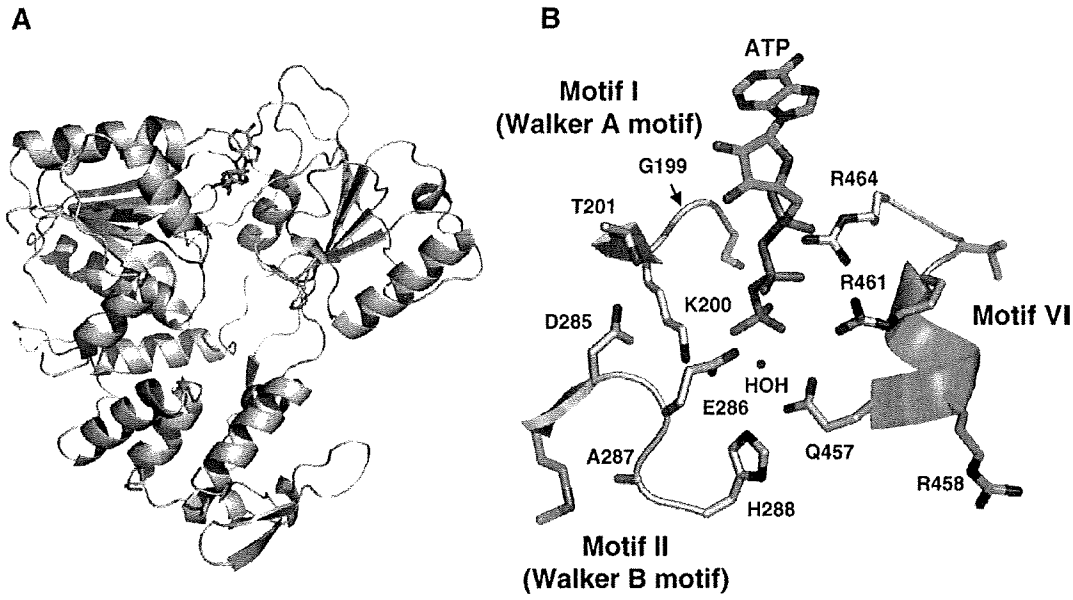

Fig. 2. A hypothetical ATP-binding model of the JEV helicase/NTPase. (A) Overall structure of the JEV helicase/NTPase domain with an ATP molecule. Orientation of the structure is identical with the Fig. 1C. The ATP molecule is localized in the cleft between the domains 1 and 2. (B) An ATP-binding pocket formed by the motifs I, II and IV. The residues consist of the ATP-binding pocket are indicated by colored atoms (C, gray; N, blue; O, red). An ATP molecule is indicated by colored atoms (C, green; N, blue; O, red; P, orange). Lys^{200} recognizes β-or γ -phosphate of ATP and forms a salt bridge with Asp^{285} and Glu^{286} for stabilization of the active site structure. Arg^{461} and Arg^{464} in motif VI form an arginine finger, work as sensors recognizing the γ-, β- and α-phosphate of ATP, respectively. The water molecule is coordinated by residues Glu^{286}, His^{288} and Gln^{457}. His^{288} is essential for the RNA-unwinding activity.

members of the family *Flaviviridae*, the structure of HCV helicase has been resolved as a helicase–nucleic acid complex (Kim et al., 1998), in which an oligomer (dU)8 is bound to the cleft between domain 3 and domains 1 and 2, with the 5′ and 3′ ends beneath the domains 2 and 1, respectively. The crystal structures of other helicases resolved with nucleic acids are superfamily 1 helicases PcrA and Rep in which a DNA duplex is bound along the side of the protein shared by domain 2 and the analog of domain 3 (Korolev et al., 1997; Velankar et al., 1999). Based on the common binding orientation in these complexes, we assumed that a single-stranded RNA proceeds through the major inter-domain cleft of the flavivirus helicase from the domain 2 side toward the domain 1 side of the protein. The structure of JEV helicase reveals that one surface has a rigid structure composed of α-helices and β-strands forming a long tunnel surrounded by residues emanating from the three domains that cross the center of the face, whereas the other surface is more negatively charged (Fig. 3). This tunnel is lined with a number of positively charged residues, with several basic patches able to accommodate a single-stranded nucleic acid, but not a duplex. JEV helicase contains an unusually high proportion of charged residues and the distribution of these residues on its surface is asymmetric just as in DEN, YFV and HCV (Wu et al., 2005; Xu et al., 2005; Yao et al., 1997). These data suggest that electrostatic repulsion might be involved in the RNA winding.

Comparison of flavivirus helicases

Previous structural analyses of the helicases of DEN, YFV, and HCV revealed that these viral helicases have highly similar structures consisting of three functional domains (Wu et al., 2005; Xu et al., 2005; Yao et al., 1997). The amino acid sequences of the NS3 helicase domain of JEV exhibited 65%, 44% and 23% homology to those of DEN, YFV and HCV, respectively. The crystal structures of the NS3 helicases of DEN (Xu et al., 2005) and YFV (Wu et al., 2005) are similar to that of JEV but slightly different from HCV (Yao et al., 1997). The distance between domains 1 and 2 of HCV helicase is longer than that in flavivirus NS3 helicases, indicating that the HCV helicase has an ATP-binding pocket with a larger volume than other flaviviruses, and the folding of domain 3 the HCV helicase is unique while that of JEV is very similar to those of other flaviviruses, including DEN and YFV (Fig. 4A). Superposition of JEV, DEN, YFV, and HCV helicases further clarified that the HCV helicase has a unique conformation in the NTPase-binding region and domain 3 in comparison with JEV, DEN, and YFV helicases (Fig. 4B). In particular, the conformation of motifs I and II of HCV helicase were different from that of JEV, DEN, and YFV helicases (Fig. 4C). The distance between motifs I and II of Cα of HCV and the other flaviviruses were 6.7 Å and 3.5 Å, respectively. The distance of Nz of Lys^{200} in the motif I was different in 4.7 Å between JEV and HCV, suggesting that HCV helicase has a wider ATP-binding pocket than other flaviviruses. In contrast to the structure of motifs I and II, that of motif VI was well conserved among the flavivirus helicases, including HCV. Although a subtle difference is observed, the ATP-binding residues in JEV, DEN, YFV, and HCV helicases are well conserved, suggesting that flavivirus helicases possess similar mechanisms of ATP hydrolysis.

ATPase and RNA helicase activities

Amino acid residues in the motif II of JEV helicase have been already shown to be essential for RNA helicase activity (Utama et al., 2000a,b). To determine the biological significance of each amino acid residue in motifs I and VI of the JEV helicase in more detail, substitution mutants of the JEV helicase were prepared as shown in Fig. 5A. Structural analyses of helicases revealed that the amino group of Lys in the Walker A motif interacts with the phosphates of ATP and the hydroxyl of Thr or Ser in the same motif, and ligates a Mg^{2+}ion (Sengoku et al., 2006). A critical role of Gly and Lys in the Walker A motif in the enzymatic and/or biochemical functions has been reported in HCV and DEN helicases (Kim et al., 1997). First, to examine the role of Gly^{199}, Lys^{200} and Thr^{201} residues in the Walker A motif of the JEV helicase on the enzymatic activity, mutant JEV helicases, G199A, K200A and T201A, in which Ala was substituted for each amino acid residue, were prepared (Fig. 5B, left). All the mutants lost both the ATPase and helicase activities, suggesting that Gly^{199}, Lys^{200} and Thr^{201} are crucial for the enzymatic activity of JEV helicase (Fig. 5C and D). From the revealed structure of JEV helicase, it was suggested that an appropriate length of a side chain of Lys^{200} plays an important role in the electrostatic interaction with the substrate in NTP hydrolysis. To examine the role of the side chain of Lys^{200} on the enzymatic activity of JEV helicase, we constructed mutant JEV helicases, K200R, K200Q, K200N, K200D, K200E and K200H, in which the polar amino acid residues, Arg, Gln, Asn, Asp, Glu and His were substituted for Lys^{200} in the Walker A motif, respectively. Although SDS-PAGE analysis verified that the mutant helicase proteins had purities and loading quantities similar to the wild type helicase (Fig. 5B), neither ATPase nor RNA helicase activity was detected in the mutant proteins (Fig. 5C and D), suggesting that Lys^{200} in the ATP-binding pocket is an indispensable amino acid and plays a critical role in the enzymatic activity of JEV helicase by providing a side chain with an adequate charge and length to fit with the substrate.

The Arg^{461} and Arg^{464} within the arginine finger ($xR^{458}xG^{460}R^{461}xxR^{464}$) in the motif VI were suggested to be the active sites of ATP hydrolysis (Ahmadian et al., 1997). To further examine the role of the amino acid residues in the motif VI in ATP hydrolysis and RNA unwinding in more detail, we constructed a series of Ala substitution mutants, Q457A, R458A, R459A, G460A, R461A, V462A, G463A, and R464A (Fig. 5B, right). The R461A and R464A mutants completely lost ATPase activity and the Q457A and R458A mutants exhibited 80% and 90% reduction of ATPase activity, respectively (Fig. 5C), whereas all four of these mutants lost RNA helicase activity (Fig. 5D). These results suggest that Gln^{457}, Arg^{461} and Arg^{464} in the ATP-binding pocket participate in the enzymatic activities of JEV helicase by interacting with the substrate, and Arg^{458}, which is located outside of the ATP-binding pocket, may help to support the helix conformation of motif VI in an enzymatically active state. Although the conserved amino acid residues in the arginine finger were suggested to be essential for enzymatic activity, substitution of Ala for Gly^{460} had no effect on either ATPase or RNA-unwinding activities, as seen in the mutants in which non-conserved amino acid residues such as Gly^{463}, Val^{462} and Arg^{459} were substituted for Ala, suggesting that Gly^{460} does not play an important role in the enzymatic activity of JEV helicase. To

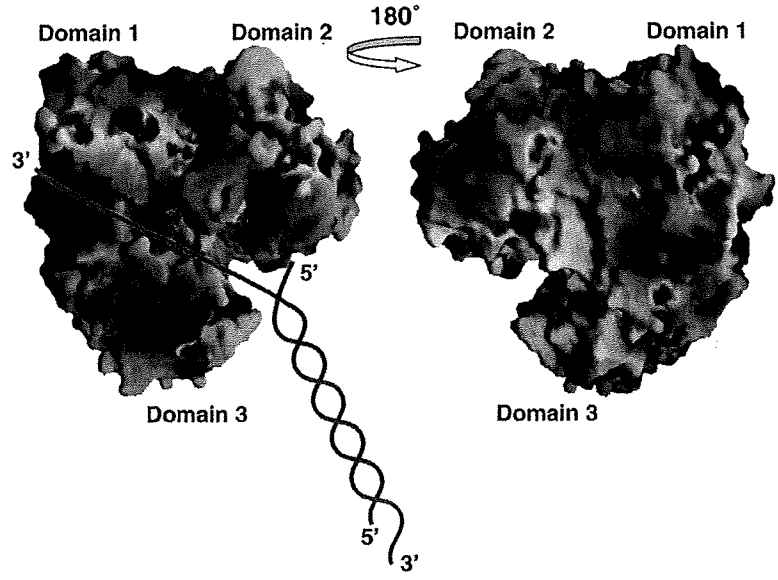

Fig. 3. Surface representation of the JEV NS3 helicase/NTPase domain. The left panel shows a nucleotide-binding face exhibiting a rigid structure composed of α-helices and β-strands and forming a long tunnel surrounded by residues emanating from the three domains that across the center of the face. Positive electrostatic potentials are colored blue and negative ones are colored red. The right panel provides a view of the other surface rotated by 180° around a vertical axis exhibiting a flat structure consisting of more negatively charged. The proposed binding groove for an RNA substrate (pink lines) is shown.

further examine the effect of mutations in the helicase on the replication of JEV, we constructed full-length JEV genomic RNAs in which the amino acid residues in motifs I and VI were substituted. Mutations in the JEV helicase abrogating the enzymatic activities are lethal and no infectious virus was recovered (G199A, K200A, T201A, Q457A, R458A, R461A, and R464A) upon transfection of the full-length RNA into Vero cells, whereas infectious viruses were recovered upon transfection with RNA of the wild type and the G460A mutant possessing the enzymatic activities (data not shown). These results suggest that the amino acids in motifs I and VI participating in the ATPase/helicase activity are indispensable for viral replication as reported in DEN (Matusan et al., 2001).

Discussion

All viruses are thought to functionally require helicase for their replication. In general, most RNA viruses that replicate primarily in the cytoplasm carry a self-encoding helicase, whereas DNA viruses that replicate primarily in the nucleus often utilize a cellular helicase (Kwong et al., 2005). In this study we determined the crystal structure of the JEV NS3 helicase/NTPase domain and investigated the roles of the amino acids in the conserved sequence motifs on the enzymatic activities and virus replication. With respect to the overall structure, JEV helicase exhibited a three-dimensional structure that was similar to the DEN and YFV helicases, but was slightly different from that of the HCV helicase in the ATP-binding pocket and domain 3.

The motif I or Walker A motif is conserved in all three helicase superfamilies and involved in the binding to the β or γ phosphate group of NTPs. The motif II or Walker B motif is also present in all the superfamilies and predicted to bind to Mg^{2+}, forming a complex with the terminal phosphates of the NTPs. The signature NTP-binding sequence GSGKT, is located at the N-terminus of the α-helix in the Walker A motif and in close proximity to an invariant Asp localized within the DExH box in the Walker B motif. In the absence of substrate, the side chains of the Walker A and B motifs formed hydrogen bonds with each other and also with residues within a conserved TATPP sequence in the motif III. Interactions included a salt bridge between Lys and Asp side chains between Walker A and B

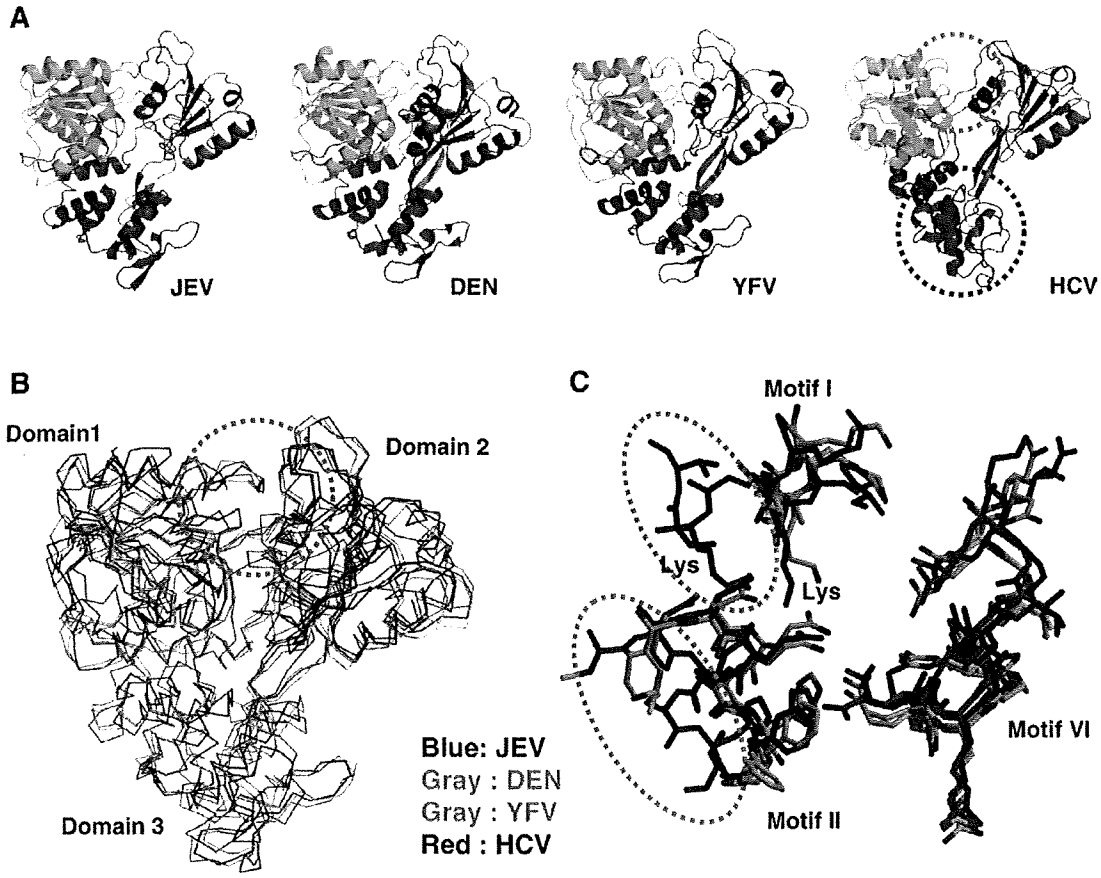

Fig. 4. Comparison of flavivirus NS3 helicase/NTPase domains. (A) Crystal structures of the NS3 helicase/NTPase domains of JEV, DEN (Protein Data Bank accession code 2BHR), YFV (Protein Data Bank accession code 1YKS) and HCV (Protein Data Bank accession code 1HEI). (B) Superimposition of each of helicase/NTPase domain. Gray: DEN and YFV; red: HCV; blue: JEV. (C) Superimposition of motifs I, II and VI. The side chains are indicated by colored atoms (C: gray; N: blue; O: red).

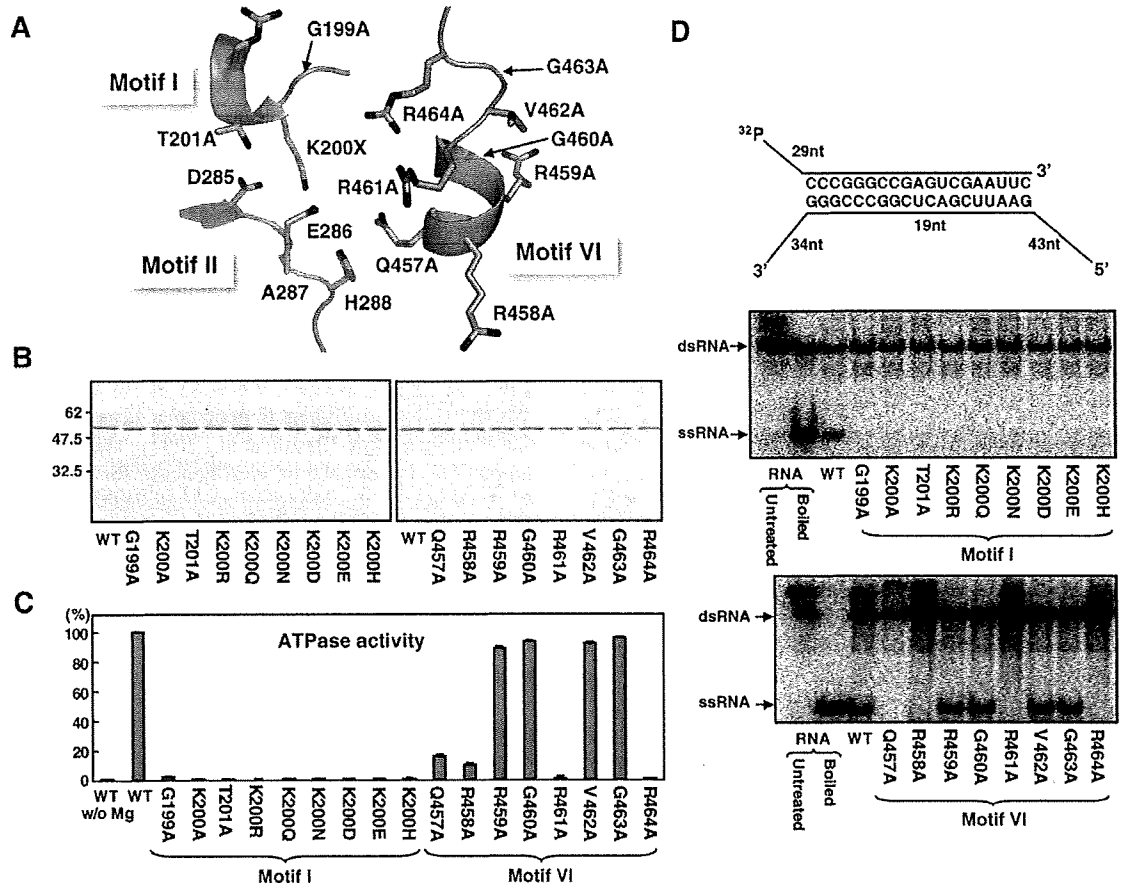

Fig. 5. ATPase and RNA helicase activities of the JEV NS3 helicase/NTPase domain. (A) Mutations introduced into amino acid residues of motif I (red) and motif VI (blue). (B) SDS-PAGE analysis of the purified JEV NS3 helicase/NTPase domain. One μg of the wild type or mutant proteins was subjected to SDS-PAGE and stained with Coomassie brilliant blue. The molecular mass of the JEV NS3 helicase/NTPase domain was about 54 kDa. (C) ATPase activities of the wild type and mutant proteins. The colorimetric NTPase assay was conducted by measuring the amount of free phosphate moiety release from nucleoside triphosphate as described in the Materials and methods. WT w/o Mg means ATPase activity of WT helicase in the absence of Mg^{2+}. The value obtained by using the wild type helicase is defined as 100%. (D) RNA helicase activities of wild type and mutant proteins. A schematic representation of the dsRNA substrate used in the unwinding assay is shown at the top of the figure. The representative images of RNA helicase assays are shown at the middle and bottom. The substrate dsRNA and unwinding ssRNA are indicated by arrows.

motifs. Structural comparisons identified the TATPP sequence located at the end of the β-strand between Walker A and B motifs and suggested that this sequence made up part of the 'switch region' responsible for the transition of conformational changes upon NTP hydrolysis (Kim et al., 1998).

Based on the crystal structure of JEV helicase, Lys^{200} is a polarity residue projecting into the ATP-binding pocket in motif I, suggesting that Lys^{200} interacts with β or γ-phosphate of ATP. We therefore constructed mutant helicases in which Lys^{200} was substituted for several other polarity residues. We speculated that a substitution of Lys^{200} for Arg retains the ATPase and RNA-unwinding activities, because both Lys and Arg are positively charged residues; however all mutants completely lost the enzymatic activities. These results suggest that Lys^{200} in motif I is indispensable for the activity due to its adequate polarity and sufficiently long side chain as well as its failure form a salt bridge with Asp^{285} and Glu^{286}. Although the other residues, Gly^{199} and Thr^{201}, in motif I do not have side chains to interact with the substrate, replacing these residues with Ala also abrogated the activity. In PcrA and Vasa, Thr in motif I was coordinated with Mg^{2+}(Sengoku et al., 2006; Velankar et al., 1999), suggesting that Gly^{199} and Thr^{201} in JEV helicase are important to sustain the conformation of the Walker A motif and that Mg^{2+}may be coordinated with Thr^{201} via an arrangement mediated by water.

The motif II or Walker B motif has a DEx(D/H) sequence known as the ATP-binding motif, and mutation analyses revealed that any residues would be accommodated in the *x* position (Marians, 1997). JEV helicase, a bovine diarrhea disease virus NS3 protein, HCV helicase, and *E. coli* UvrB have Ala, Tyr, Cys and Ser residues at the *x* position, respectively (Nakagawa et al., 1997). Previous mutational analyses in the DEAH motif of JEV helicase revealed that Asp^{285} and Glu^{286} in the motif were essential for both ATPase and RNA helicase activities, whereas Ala^{287} and His^{288} in the motif were indispensable for RNA helicase activity but not for ATPase activity (Utama et al.,

2000a). Ala^{287} in the DEAH motif lacks a side chain interacting with substrate, and we therefore speculate that Asp^{285} coordinates Mg^{2+} via a mediating by water, and Asp^{285} and Ala^{287} are important to sustain the conformation of motif II by forming salt bridge with Lys^{200}. Although His^{288} is too far away to be considered an active site, our structural analyses suggest that His^{288} in the DEAH motif is required for helicase activity and plays a role in the NTP hydrolysis reaction by mediating the water.

The mutant JEV helicases in which Ala was substituted for Gln^{457}, Arg^{458}, Arg^{461} or Arg^{464} in the active site of motif VI, but not those in which Ala was substituted for Arg^{459}, Gly^{460}, Val^{462} or Gly^{463}, exhibited a drastic reduction in the ATPase and helicase activities. Mutations of Arg in the motif VI of HCV helicase completely abrogated both ATPase and helicase activities (Kim et al., 1997), and R457A and R458A mutants of DEN helicase retained the NTPase activity but lost the RNA-unwinding activity (Matusan et al., 2001). However, a full-length DEN NS3 mutant in which Ala was substituted for Arg^{457} and Arg^{458} exhibited a severe reduction in ATPase activity, but a two-fold increase in the helicase activity. The discrepancy in DEN helicase activity might be attributable to an approximately 30-fold higher activity in the full-length NS3 protein than in the N-terminally truncated helicase protein (Li et al., 1999a). Arg^{461} and Arg^{464} of JEV helicase interact with γ-and α -phosphate of ATP respectively, and Gln^{457} also interacts with γ-phosphate of ATP and coordinates water for NTPase hydrolysis with His^{288}. These results suggest that the arginine finger in motif VI of JEV helicase works as a sensor of substrate recognition and the binding pocket of NTPs plays an important role in the interaction with water, substrates and divalent cations.

The crystal structure of JEV helicase revealed a tunnel lined with a number of basic residues sufficient for accommodating a single-stranded nucleic acid. A conserved Trp^{501} in domain 3 of HCV helicase is stacked with one of the bases of the nucleic acid and is required for its RNA helicase activity, and ATP binding and hydrolysis are suggested to cause rotation of domain 2 relative to domains 1 and 3, which leads to translocation of the protein by one or two bases as the protein ratchets like an inchworm along the strand below domains 1 and 2 (Kim et al., 1998; Kim et al., 2003). In contrast to HCV helicase, flavivirus helicases have no conserved aromatic residue at either end of the presumed single-stranded RNA-binding cleft. In DEN helicase, the pocket next to Ile^{365} could act as a 'helix opener' by disrupting hydrogen bonds at the fork, and the basic concave face between domains II and III would act as a 'translocator' by binding dsRNA ahead of the fork (Sampath et al., 2006). Helicases catalyze various functions such as unwinding the strands of double-helical DNA, removing secondary structures in RNA, and displacing proteins bound to nucleic acid by moving along the nucleic acid unidirectionally either in the 5′ to 3′ or the 3′ to 5′ direction. HCV helicase binds to a substrate with a five-base ssDNA tail at the 3′ end 50 times tighter than a similar substrate with a five-base tail at the 5′ end and unwinds substrates in the 3′ to 5′ direction (Levin et al., 2005). Therefore, JEV helicase structurally similar to HCV helicase may translocate dsRNA in the 3′ to 5′ direction.

In JEV helicase, residues interacting with the phosphodiester backbone may include Arg^{226} (motif Ia), Lys^{367} (motif IV), Arg^{388}, Lys^{389}, Arg^{539} and Arg^{609} These residues are well conserved in helicases of DEN and YFV, suggesting that residues that participate in the RNA unwinding of flavivirus helicase are different from HCV helicases.

Although the motifs in the active sites of the RNA helicases are well conserved among flaviviruses, HCV, WNV and JEV helicases exhibited a divergent sensitivity to the inhibitors (Borowski et al., 2003), suggesting that these differences are obtained during the evolutional adaptation of each virus to their hosts. Very recently, a single amino acid substitution of Pro for Thr^{249} in the NS3 helicase in a WNV strain with low virulence was shown to be sufficient to generate a virus highly virulent to the American crow (Brault et al., 2007). These results further support the importance of viral helicase for the adaptation of RNA viruses to the changing environment. Many RNA helicases remain to be investigated and further structural analyses of the RNA helicases will provide clues for the development of broad-spectrum or specific antiviral drugs for the treatment of flavivirus infection.

Materials and methods

Expression and purification of JEV NS3 helicase/NTPase

A cDNA encoding the JEV helicase/NTPase domain (amino acid residues 171 to 619 of the AT31 strain) was amplified by polymerase chain reaction (PCR) with the synthetic DNA primers, 5′-AAGAATTCAGCGCCATCGTGCAGGGTGA-3′ and 5′-AACTCGAGTCTCTTTCCTGCTGC-3′. A 1.4 kb region of the PCR-amplified DNA fragment was digested with EcoRI and XhoI, and cloned into the corresponding cloning sites of the *E. coli* expression vector, pET21b (Novagen, San Diego, CA). The expression product is composed of 449 amino acid residues of JEV NS3 helicase/NTPase with the vector-derived 14 amino acid residues at the N-terminus and 6 amino acid residues containing a His-tag (histidine hexamaer) at the C-terminus. The His-tagged JEV helicase/NTPase was expressed in the *E. coli* BL21 (DE3) pLysS strain in the presence of 1 mM isopropyl β-thiogalactoside for 5 h at 20 °C and the bacteria were sonicated in a buffer [20 mM Tris–HCl (pH 8.0) and 500 mM NaCl] with 40 mM imidazole. After centrifugation, the supernatant was applied to a NiTrap HP column (GE Healthcare, Tokyo, Japan) and the resulting nickel-binding proteins were eluted under a linear gradient of 40–400 mM imidazole in the same buffer. After passage through a gel filtration column (HiLoad 16/60 Superdex 200 pg; GE Healthcare), the recombinant protein was applied to an anion exchange column (HiTrap Q; GE Healthcare) and eluted under a linear gradient of 100–400 mM NaCl in 20 mM Tris–HCl buffer (pH 8.0). The final product consists of 469 amino acid residues containing the JEV NS3 NTPase/helicase domain flanked by 14 and 6 amino acid residues at the N-and C-terminus, respectively. Substitution of Ala for the JEV helicase at amino acid residues Gly^{199}, Lys^{200}, Thr^{201}, Gln^{457}, Arg^{458}, Arg^{459}, Gly^{460}, Arg^{461}, Val^{462}, Gly^{463} and Arg^{464}, and mutation at residue Lys^{200} to

Arg, Gln, Asn, Asp, Glu, and His, respectively, were accomplished by PCR-based mutagenesis.

ATPase assay

The colorimetric NTPase assay was conducted by measuring the amount of free phosphate moiety released from nucleoside triphosphate as described previously with minor modifications (Xu et al., 2005). Briefly, 50 μl per well of a reaction mixture containing 10 mM MOPS buffer (pH 6.5), 2 mM NTP, 1 mM $MgCl_2$ and 0.1 μg of purified JEV NS3 NTPase/helicase protein was incubated in a 96-well plate at room temperature for 30 min, and 100 μl of dye solution (water: 0.081% malachite green in water: 5.7% ammonium molybdate in 6 N HCl: 2.3% polyvinylalchol in water=2:2:1:1, v/v) was added. Color development was terminated by addition of 25 μl of 30% sodium citrate after 5 min of incubation, and the absorbance at 620 nm was determined.

RNA helicase assay

The labeled single-stranded RNA fragment was synthesized by Riboprobe Systems (Promega, Madison, WI) using a pSP72 DNA fragment linearized with BamHI as a template in the presence of [α-^{32}P]UTP (3000 Ci/mmol; GE Healthcare). Plasmid pGEM-3Zf(+) (Promega) was linearized with EaeI and non-labeled RNA fragment was prepared. The RNA transcripts were resuspended in 100 μl of annealing buffer [10 mM Tris–HCl (pH 8.5), 100 mM NaCl, 8 fmol of each transcript], boiled for 5 min and hybridized at room temperature overnight. Schematic representation of the double-stranded RNA substrate is shown in Fig. 5D. The RNA helicase assay was carried out in 20 μl of helicase buffer containing 25 mM MES (pH 6.0), 2 mM DTT, 2 mM $MgCl_2$, 5 mM ATP, 1.25 U of RNase inhibitor (Promega), 0.32 fmol of the RNA substrate and 0.1 μg of purified JEV NS3 NTPase/helicase protein at 37 °C for 30 min. The reaction was terminated with 5 μl of loading buffer [100 mM Tris–HCl (pH 7.4), 5 mM EDTA, 0.5% SDS, 50% glycerol, 0.1% xylene cyanol, 0.1% bromophenol blue] and analyzed by 10% native polyacrylamide gel electrophoresis (PAGE). The autoradiographic pattern was obtained by using a BAS 1500 Image Analyzing System (Fujifilm, Tokyo, Japan).

Crystallization of JEV NS3 helicase/NTPase

Crystallization of the JEV NS3 helicase/NTPase domain was carried out under conditions screened by the hanging-drop vapor-diffusion method by Wizard I and II kits (Emerald BioSystems, Bainbridge Island, WA). The purified protein solution (2 μl) at a concentration of 10 mg/ml in a buffer [20 mM Tris–HCl (pH 8.0) and 250 mM NaCl] was equilibrated with 0.4 ml of a reservoir solution containing 15% ethanol and 100 mM Tris–HCl (pH 7.0) at 25 °C. The size and quality of the crystals were further improved by an addition of 4% pentaerythritol etoxylate (3/4 EO/OH). As a result, single crystals with dimensions of 0.5 × 0.3 × 0.2 mm were obtained in the drop after 5 days of incubation (Fig. 1B).

Data collection and processing

The crystal of the JEV NS3 helicase/NTPase domain was soaked in the reservoir solution with 30% (w/v) glycerol for 1 min and mounted in nylon CryoLoops (Hampton Research, Aliso Viejo, CA). Then, it was placed directly into a nitrogen stream at 100K. Data were collected at a beamline BL44XU of SPring-8 (Hyogo, Japan) using a DIP6040 imaging plate (Mac Science, Yokohama, Japan). The oscillation ranges were 200° with oscillations per frame being 1°. Oscillation data were recorded in frame 1° oscillation with 3-second exposure time for each image. The data were processed using the computer program HKL2000. The statistics of the diffraction data are summarized in Table 1. The space group was determined to be monoclinic $P2_1$. Assuming that there is one molecule of JEV NS3 helicase/NTPase domain in the asymmetric unit, the value of the Matthews content V_M (Matthews, 1968) is 2.2 $Å^3$ Da^{-1}, corresponding to a solvent content of 48%, both of which are within the normal range of values for protein crystals (Matthews, 1968).

Phasing model building, structure refinement, and analysis

The structure model was determined by the molecular replacement method using Molrep (Vagin and Teplyakov, 2000). The DEN helicase/NTPase domain (Protein Data Bank entry 2BHR) (Xu et al., 2005) was used as an initial search model. All refinement were carried out using REFMAC (Murshudov et al., 1997). About 50% of the model was autobuilt into the 1.8 Å electron density using wARP (Perrakis et al., 1997). An essential complete model was built into this map with program O (Jones et al., 1991). The refined model consisted of JEV helicase/NTPase domain in an asymmetric unit. The final coordinates and structure factor have been submitted to the Protein Data Bank with accession number 2Z83. In a final model, four regions, amino acid residues 171 to 180, 245 to 254, 274 to 276 and 412 to 416, are disordered and not included. No residues are in the disallowed region of the Ramachandoran plot. The final statistics are summarized in Table 1. Figs. 1C, 2, 3, and 5A were drawn by using the program PyMol and Fig. 4 was drawn using Molscript (Esnouf, 1999) and Raster 3D (Merritt and Murphy, 1994). The superposition of the structure and calculation of the root mean square (RMS) deviation were carried out using the program LASQKAB from the CCP4 suite (Collaborative Computational Project Number 4, 1994). We calculated the electrostatic potentials of the JEV helicase/NTPase domain by GRASP program (Nicholls et al., 1991).

Hypothetical ATP-binding model

An ATP-binding model of the JEV helicase domain was built with O (Jones et al., 1991) The structural data of the ATP molecule was obtained from a PDB file, 1xdn.

Generation of JEV from plasmid

As described above, mutations in the JEV helicase were introduced in the plasmid pMWJEATG1 carrying a full-length

cDNA of the JEV AT31 strain under the control of a T7 promoter (Zhao et al., 2005) by PCR-based mutagenesis. The plasmid DNAs encoding the wild type or mutant JEVs digested with KpnI were used as templates for RNA synthesis. Capped, full-length JEV RNAs were synthesized *in vitro* by an mMESSAGE mMACHINE T7 kit (Ambion, Austin, TX), purified by precipitation with lithium chloride, and used for electroporation into Vero (African green monkey kidney) cells maintained in Dulbecco's modified Eagle's minimal essential medium supplemented with 10% fetal bovine serum as described previously (Mori et al., 2005).

Acknowledgments

We thank H. Murase for her secretarial work. We also thank the staff of SPring-8 BL44XU beamline for their assistance with the data collection. This work was supported in part by grants-in-aid from the Ministry of Health, Labor and Welfare; the 21st Century Center of Excellence Program of Japan; the Ministry of Education, Culture, Sports, Science and Technology of Japan; the Foundation for Research Collaboration Center on Emerging and Re-emerging Infections; and the Zoonoses Control Project of the Ministry of Agriculture, Forestry and Fisheries of Japan.

References

Ahmadian, M.R., Stege, P., Scheffzek, K., Wittinghofer, A., 1997. Confirmation of the arginine-finger hypothesis for the GAP-stimulated GTP-hydrolysis reaction of Ras. Nat. Struct. Biol. 4, 686–689.

Borowski, P., Deinert, J., Schalinski, S., Bretner, M., Ginalski, K., Kulikowski, T., Shugar, D., 2003. Halogenated benzimidazoles and benzotriazoles as inhibitors of the NTPase/helicase activities of hepatitis C and related viruses. Eur. J. Biochem. 270, 1645–1653.

Brault, A.C., Huang, C.Y., Langevin, S.A., Kinney, R.M., Bowen, R.A., Ramey, W.N., Panella, N.A., Holmes, E.C., Powers, A.M., Miller, B.R., 2007. A single positively selected West Nile viral mutation confers increased virogenesis in American crows. Nat. Genet. 39, 1162–1166.

Caruthers, J.M., McKay, D.B., 2002. Helicase structure and mechanism. Curr. Opin. Struct. Biol. 12, 123–133.

Cho, H.S., Ha, N.C., Kang, L.W., Chung, K.M., Back, S.H., Jang, S.K., Oh, B.H., 1998. Crystal structure of RNA helicase from genotype 1b hepatitis C virus. A feasible mechanism of unwinding duplex RNA. J. Biol. Chem. 273, 15045–15052.

Collaborative Computational Project Number 4, 1994. The CCP4 suite: programs for protein crystallography. Acta Crystallogr. D. Biol. Crystallogr. 50, 760–763.

Cui, T., Sugrue, R.J., Xu, Q., Lee, A.K., Chan, Y.C., Fu, J., 1998. Recombinant dengue virus type 1 NS3 protein exhibits specific viral RNA binding and NTPase activity regulated by the NS5 protein. Virology 246, 409–417.

Esnouf, R.M., 1999. Further additions to MolScript version 1.4, including reading and contouring of electron-density maps. Acta Crystallogr. D. Biol. Crystallogr. 55, 938–940.

Jones, T.A., Zou, J.Y., Cowan, S.W., Kjeldgaard, 1991. Improved methods for building protein models in electron density maps and the location of errors in these models. Acta Crystallogr. A. 47, 110–119.

Kim, D.W., Kim, J., Gwack, Y., Han, J.H., Choe, J., 1997. Mutational analysis of the hepatitis C virus RNA helicase. J. Virol. 71, 9400–9409.

Kim, J.L., Morgenstern, K.A., Griffith, J.P., Dwyer, M.D., Thomson, J.A., Murcko, M.A., Lin, C., Caron, P.R., 1998. Hepatitis C virus NS3 RNA helicase domain with a bound oligonucleotide: the crystal structure provides insights into the mode of unwinding. Structure 6, 89–100.

Kim, J.W., Seo, M.Y., Shelat, A., Kim, C.S., Kwon, T.W., Lu, H.H., Moustakas, D.T., Sun, J., Han, J.H., 2003. Structurally conserved amino Acid w501 is required for RNA helicase activity but is not essential for DNA helicase activity of hepatitis C virus NS3 protein. J. Virol. 77, 571–582.

Koonin, E.V., 1991. Similarities in RNA helicases. Nature 352, 290.

Korolev, S., Hsieh, J., Gauss, G.H., Lohman, T.M., Waksman, G., 1997. Major domain swiveling revealed by the crystal structures of complexes of *E. coli* Rep helicase bound to single-stranded DNA and ADP. Cell 90, 635–647.

Kuo, M.D., Chin, C., Hsu, S.L., Shiao, J.Y., Wang, T.M., Lin, J.H., 1996. Characterization of the NTPase activity of Japanese encephalitis virus NS3 protein. J. Gen. Virol. 77, 2077–2084.

Kwong, A.D., Rao, B.G., Jeang, K.T., 2005. Viral and cellular RNA helicases as antiviral targets. Nat. Rev. Drug Discov. 4, 845–853.

Levin, M.K., Gurjar, M., Patel, S.S., 2005. A Brownian motor mechanism of translocation and strand separation by hepatitis C virus helicase. Nat. Struct. Mol. Biol. 12, 429–435.

Li, H., Clum, S., You, S., Ebner, K.E., Padmanabhan, R., 1999a. The serine protease and RNA-stimulated nucleoside triphosphatase and RNA helicase functional domains of dengue virus type 2 NS3 converge within a region of 20 amino acids. J. Virol. 73, 3108–3116.

Li, J., Tang, H., Mullen, T.M., Westberg, C., Reddy, T.R., Rose, D.W., Wong-Staal, F., 1999b. A role for RNA helicase A in post-transcriptional regulation of HIV type 1. Proc. Natl. Acad. Sci. U. S. A. 96, 709–714.

Luking, A., Stahl, U., Schmidt, U., 1998. The protein family of RNA helicases. Crit. Rev. Biochem. Mol. Biol. 33, 259–296.

Marians, K.J., 1997. Helicase structures: a new twist on DNA unwinding. Structure 5, 1129–1134.

Matthews, B.W., 1968. Solvent content of protein crystals. J. Mol. Biol. 33, 491–497.

Matusan, A.E., Kelley, P.G., Pryor, M.J., Whisstock, J.C., Davidson, A.D., Wright, P.J., 2001. Mutagenesis of the dengue virus type 2 NS3 proteinase and the production of growth-restricted virus. J. Gen. Virol. 82, 1647–1656.

Merritt, E.A., Murphy, M.E., 1994. Raster3D Version 2.0. A program for photorealistic molecular graphics. Acta Crystallogr. D. Biol. Crystallogr. 50, 869–873.

Mori, Y., Okabayashi, T., Yamashita, T., Zhao, Z., Wakita, T., Yasui, K., Hasebe, F., Tadano, M., Konishi, E., Moriishi, K., Matsuura, Y., 2005. Nuclear localization of Japanese encephalitis virus core protein enhances viral replication. J. Virol. 79, 3448–3458.

Murshudov, G.N., Vagin, A.A., Dodson, E.J., 1997. Refinement of macromolecular structures by the maximum-likelihood method. Acta Crystallogr. D. Biol. Crystallogr. 53, 240–255.

Nakagawa, N., Masui, R., Kato, R., Kuramitsu, S., 1997. Domain structure of *Thermus thermophilus* UvrB protein. Similarity in domain structure to a helicase. J. Biol. Chem. 272, 22703–22713.

Nicholls, A., Sharp, K.A., Honig, B., 1991. Protein folding and association: insights from the interfacial and thermodynamic properties of hydrocarbons. Proteins 11, 281–296.

Niedenzu, T., Roleke, D., Bains, G., Scherzinger, E., Saenger, W., 2001. Crystal structure of the hexameric replicative helicase RepA of plasmid RSF1010. J. Mol. Biol. 306, 479–487.

Perrakis, A., Sixma, T.K., Wilson, K.S., Lamzin, V.S., 1997. wARP: improvement and extension of crystallographic phases by weighted averaging of multiple-refined dummy atomic models. Acta Crystallogr. D. Biol. Crystallogr. 53, 448–455.

Sampath, A., Xu, T., Chao, A., Luo, D., Lescar, J., Vasudevan, S.G., 2006. Structure-based mutational analysis of the NS3 helicase from dengue virus. J. Virol. 80, 6686–6690.

Schmid, S.R., Linder, P., 1992. D-E-A-D protein family of putative RNA helicases. Mol. Microbiol. 6, 283–291.

Sengoku, T., Nureki, O., Nakamura, A., Kobayashi, S., Yokoyama, S., 2006. Structural basis for RNA unwinding by the DEAD-box protein *Drosophila* Vasa. Cell 125, 287–300.

Solomon, T., Ni, H., Beasley, D.W., Ekkelenkamp, M., Cardosa, M.J., Barrett, A.D., 2003. Origin and evolution of Japanese encephalitis virus in southeast Asia. J. Virol. 77, 3091–3098.

Subramanya, H.S., Bird, L.E., Brannigan, J.A., Wigley, D.B., 1996. Crystal structure of a DExx box DNA helicase. Nature 384, 379–383.

Sumiyoshi, H., Mori, C., Fuke, I., Morita, K., Kuhara, S., Kondou, J., Kikuchi, Y., Nagamatu, H., Igarashi, A., 1987. Complete nucleotide sequence of the Japanese encephalitis virus genome RNA. Virology 161, 497–510.

Tanner, N.K., Cordin, O., Banroques, J., Doere, M., Linder, P., 2003. The Q motif: a newly identified motif in DEAD box helicases may regulate ATP binding and hydrolysis. Mol. Cell 11, 127–138.

Theis, K., Chen, P.J., Skorvaga, M., Van Houten, B., Kisker, C., 1999. Crystal structure of UvrB, a DNA helicase adapted for nucleotide excision repair. Embo J. 18, 6899–6907.

Tsai, T.F., 2000. New initiatives for the control of Japanese encephalitis by vaccination: minutes of a WHO/CVI meeting, Bangkok, Thailand, 13–15 October 1998. Vaccine 18 (Suppl 2), 1–25.

Utama, A., Shimizu, H., Hasebe, F., Morita, K., Igarashi, A., Shoji, I., Matsuura, Y., Hatsu, M., Takamizawa, K., Hagiwara, A., Miyamura, T., 2000a. Role of the DExH motif of the Japanese encephalitis virus and hepatitis C virus NS3 proteins in the ATPase and RNA helicase activities. Virology 273, 316–324.

Utama, A., Shimizu, H., Morikawa, S., Hasebe, F., Morita, K., Igarashi, A., Hatsu, M., Takamizawa, K., Miyamura, T., 2000b. Identification and characterization of the RNA helicase activity of Japanese encephalitis virus NS3 protein. FEBS Lett. 465, 74–78.

Vagin, A., Teplyakov, A., 2000. An approach to multi-copy search in molecular replacement. Acta Crystallogr. D. Biol. Crystallogr. 56, 1622–1624.

Velankar, S.S., Soultanas, P., Dillingham, M.S., Subramanya, H.S., Wigley, D.B., 1999. Crystal structures of complexes of PcrA DNA helicase with a DNA substrate indicate an inchworm mechanism. Cell 97, 75–84.

Warrener, P., Tamura, J.K., Collett, M.S., 1993. RNA-stimulated NTPase activity associated with yellow fever virus NS3 protein expressed in bacteria. J. Virol. 67, 989–996.

Wengler, G., Wengler, G., 1991. The carboxy-terminal part of the NS 3 protein of the West Nile flavivirus can be isolated as a soluble protein after proteolytic cleavage and represents an RNA-stimulated NTPase. Virology 184, 707–715.

Wu, J., Bera, A.K., Kuhn, R.J., Smith, J.L., 2005. Structure of the flavivirus helicase: implications for catalytic activity, protein interactions, and proteolytic processing. J. Virol. 79, 10268–10277.

Xu, T., Sampath, A., Chao, A., Wen, D., Nanao, M., Chene, P., Vasudevan, S.G., Lescar, J., 2005. Structure of the Dengue virus helicase/nucleoside triphosphatase catalytic domain at a resolution of 2.4 A. J. Virol. 79, 10278–10288.

Yao, N., Hesson, T., Cable, M., Hong, Z., Kwong, A.D., Le, H.V., Weber, P.C., 1997. Structure of the hepatitis C virus RNA helicase domain. Nat. Struct. Biol. 4, 463–467.

Yao, N., Reichert, P., Taremi, S.S., Prosise, W.W., Weber, P.C., 1999. Molecular views of viral polyprotein processing revealed by the crystal structure of the hepatitis C virus bifunctional protease-helicase. Structure 7, 1353–1363.

Zhao, Z., Date, T., Li, Y., Kato, T., Miyamoto, M., Yasui, K., Wakita, T., 2005. Characterization of the E-138 (Glu/Lys) mutation in Japanese encephalitis virus by using a stable, full-length, infectious cDNA clone. J. Gen. Virol. 86, 2209–2220.

JOURNAL OF VIROLOGY, Oct. 2009, p. 10427–10436 Vol. 83, No. 20
0022-538X/09/$08.00+0 doi:10.1128/JVI.01035-09
Copyright © 2009, American Society for Microbiology. All Rights Reserved.

Cochaperone Activity of Human Butyrate-Induced Transcript 1 Facilitates Hepatitis C Virus Replication through an Hsp90-Dependent Pathway▽

Shuhei Taguwa,[1] Hiroto Kambara,[1] Hiroko Omori,[2] Hideki Tani,[1] Takayuki Abe,[1] Yoshio Mori,[1] Tetsuro Suzuki,[3] Tamotsu Yoshimori,[2] Kohji Moriishi,[1] and Yoshiharu Matsuura[1]*

Department of Molecular Virology[1] and Department of Cellular Regulation,[2] Research Institute for Microbial Diseases, Osaka University, Osaka, and Department of Virology II, National Institute of Infectious Diseases, Tokyo,[3] Japan

Received 21 May 2009/Accepted 27 July 2009

Hepatitis C virus (HCV) nonstructural protein 5A (NS5A) is a component of the replication complex consisting of several host and viral proteins. We have previously reported that human butyrate-induced transcript 1 (hB-ind1) recruits heat shock protein 90 (Hsp90) and FK506-binding protein 8 (FKBP8) to the replication complex through interaction with NS5A. To gain more insights into the biological functions of hB-ind1 in HCV replication, we assessed the potential cochaperone-like activity of hB-ind1, because it has significant homology with cochaperone p23, which regulates Hsp90 chaperone activity. The chimeric p23 in which the cochaperone domain was replaced with the p23-like domain of hB-ind1 exhibited cochaperone activity comparable to that of the authentic p23, inhibiting the glucocorticoid receptor signaling in an Hsp90-dependent manner. Conversely, the chimeric hB-ind1 in which the p23-like domain was replaced with the cochaperone domain of p23 resulted in the same level of recovery of HCV propagation as seen in the authentic hB-ind1 in cells with knockdown of the endogenous hB-ind1. Immunofluorescence analyses revealed that hB-ind1 was colocalized with NS5A, FKBP8, and double-stranded RNA in the HCV replicon cells. HCV replicon cells exhibited a more potent unfolded-protein response (UPR) than the parental and the cured cells upon treatment with an inhibitor for Hsp90. These results suggest that an Hsp90-dependent chaperone pathway incorporating hB-ind1 is involved in protein folding in the membranous web for the circumvention of the UPR and that it facilitates HCV replication.

Hepatitis C virus (HCV) is the major causative agent of non-A, non-B hepatitis in humans and infects approximately 170 million people worldwide (64). HCV belongs to the genus *Hepacivirus* of the family *Flaviviridae* and is classified into six major genotypes (39). The virus forms small, round, enveloped particles and possesses a genome consisting of a single positive-stranded RNA with a nucleotide length of 9.6 kb. The viral genome encodes a single precursor polyprotein consisting of approximately 3,000 amino acids, which in turn is posttranslationally processed into 10 viral proteins by host and viral proteases. The structural proteins are cleaved from the N-terminal one-fourth of the polyprotein by the host signal peptidase and signal peptide peptidase (36, 43, 44), resulting in the maturation of capsid protein, two envelope proteins, and viroporin p7. The nonstructural protein 2 (NS2) protease cleaves its own carboxyl terminus, and then NS3 cleaves the appropriate downstream positions to produce NS3, NS4A, NS4B, NS5A, and NS5B (24, 60), which form the replication complex, together with several host proteins (14, 35).

NS5A is a membrane-anchored zinc-binding phosphoprotein that appears to possess diverse functions, including the suppression of host defense and the regulation of virus replication (1, 15, 58), but its biological function remains unclear. Several groups, including ours, have suggested that the molecular chaperone, heat shock protein 90 (Hsp90), and several cochaperones participate in the replication complex of HCV through interaction with NS5A or other NS proteins (45, 56, 65). Hsp90 is the highly conserved and ubiquitously expressed protein that acts as a key regulator for the turnover and the activities of more than 200 signaling proteins, including steroid receptors and cell-signaling kinases (66). The chaperone activity of Hsp90 contributes to the refolding of an unfolded protein in an ATP-dependent manner, and the execution of Hsp90-dependent protein folding requires the formation of a multichaperone complex containing other chaperones (e.g., Hsp70, Hsp104, and Hsp40) and cochaperones (e.g., p23, Hop, and immunophilins) (4, 18, 48). Geldanamycin or its derivatives, which are represented as specific inhibitors of Hsp90, can destabilize and then degrade client proteins (41, 55).

The host chaperone mechanism is involved in the folding of viral polymerase to support viral replication (6, 27). Moreover, host chaperones have been reported to play roles in the assembly of viral particles and the sorting of virus proteins (9, 32, 38). We have previously reported that Hsp90 chaperone activities and chaperone-associated proteins are required for the efficient propagation of HCV (45, 56) and that human butyrate-induced transcript 1 (hB-ind1) is involved in the propagation of HCV through interactions with NS5A and Hsp90 via the coiled-coil domain and the FXXW motif, respectively (56). hB-ind1 was first reported to be a multiple-membrane-spanning protein consisting of 362 amino acids that possesses a significant homology with a cochaperones, p23, that regulates

* Corresponding author. Mailing address: Department of Molecular Virology, Research Institute for Microbial Diseases, Osaka University, 3-1, Yamadaoka, Suita-shi, Osaka 565-0871, Japan. Phone: 81-6-6879-8340. Fax: 81-6-6879-8269. E-mail: matsuura@biken.osaka-u.ac.jp.

▽ Published ahead of print on 5 August 2009.

Downloaded from jvi.asm.org at Osaka University on September 23, 2009

Hsp90 function by its cochaperone activity (11). However, the roles of hB-ind1 in the life cycle of HCV have not been precisely clarified. In this study, we investigated the role of the Hsp90-related chaperone system, including hB-ind1, in the regulation of the RNA replication and particle production of HCV.

MATERIALS AND METHODS

Plasmids. The plasmids encoding hB-ind1, NS5A, Hsp90, and FK506-binding protein 8 (FKBP8) were prepared by methods described previously (45, 56). The DNA fragments encoding hB-ind1 mutants were prepared by PCR with the introduction of a silent mutation that is resistant to the short hairpin RNA in the hB-ind1 knockdown cells, as described previously (56). The human p23 gene and glucose-regulated protein 78 (GRP78) promoter region (−151 to +22) were amplified by PCR from the total cDNA and genomic DNA of Huh7 cells, respectively. The DNA fragments encoding mutants of hB-ind1 and p23 were prepared by the method of splicing by overlap extension (26) and introduced into pEF FLAGGs pGKpuro (28). The GRP78 promoter region was introduced between the KpnI and HindIII sites of pGL3-basic (Promega, Madison, WI) and designated pGRP78-luc. The reporter plasmid carrying a firefly luciferase gene under the control of the GR promoter (pGR-luc) was purchased from Panomics (Fremont, CA). The internal-control plasmid encoding a *Renilla* luciferase (pRL-TK) was purchased from Promega. The plasmid pFK-I_{389} neo/NS3-3′/NK5.1 (47) was kindly provided by R. Bartenschlager. The plasmids used in this study were confirmed by sequencing them with an ABI Prism 3130 genetic analyzer (Applied Biosystems, Tokyo, Japan).

Cells and virus infection. All cell lines were cultured at 37°C under a humidified atmosphere and 5% CO_2. The human embryonic kidney 293T and hepatocellular carcinoma Huh7 cell lines were maintained in Dulbecco's modified Eagle's medium (DMEM) (Sigma, St. Louis, MO) supplemented with 100 U/ml penicillin, 100 μg/ml streptomycin, and 10% fetal calf serum (FCS). The human hepatocellular carcinoma cell line Huh7.5.1 was kindly provided by F. Chisari (70) and was maintained in DMEM containing nonessential amino acids, 100 U/ml penicillin, 100 μg/ml streptomycin, and 10% FCS. The Huh9-13 cell line, which is a Huh7 cell line harboring a subgenomic HCV RNA replicon (35), was maintained in DMEM containing 10% FCS, nonessential amino acids, and 1 mg/ml G418 (Nakalai Tesque, Kyoto, Japan). The hB-ind1 knockdown cell line Huh-KD and control cell line Huh-ctrl were described previously (56). Huh-KD cells were transfected with each of the expression plasmids encoding wild-type or mutant hB-ind1 and cultured for 1 week in the presence of 10 μg/ml of puromycin. The remaining cells were used for the experiments described below. The viral RNA of JFH1 was introduced into Huh7.5.1 cells according to the method of Wakita et al. (62) for preparation of the infectious HCV particles in cell culture.

Antibodies. The rabbit anti-hB-ind1 antibody was prepared as described previously (56). Mouse monoclonal antibodies to HCV NS5A, influenza virus hemagglutinin (HA) and FLAG tags, and β-actin were purchased from Austral Biologicals (San Ramon, CA), Covance (Richmond, CA), and Sigma, respectively. Mouse anti-protein disulfide isomerase (PDI) immunoglobulin G2a (IgG2a) was from Affinity Bioreagents (Golden, CO). Mouse anti-double-stranded RNA (dsRNA) IgG2a (J1 and K2) antibodies were from Biocenter Ltd. (Szirak, Hungary). Alexa Fluor 488 (AF488)-conjugated anti-mouse IgG1, AF647-conjugated anti-rabbit IgG, and AF594-conjugated anti-mouse IgG2a and IgG2b antibodies were from Invitrogen (San Diego, CA).

Transfection, immunoblotting, and immunoprecipitation. Transfection and immunoprecipitation analyses were carried out as described previously (25, 45). Immunoprecipitates boiled in loading buffer were subjected to 12.5% sodium dodecyl sulfate-polyacrylamide gel electrophoresis. The proteins were transferred to polyvinylidene difluoride membranes (Millipore, Bedford, MA) and were reacted with the appropriate antibodies. The immune complexes were visualized with Super Signal West Femto substrate (Pierce, Rockford, IL) and detected by an LAS-3000 image analyzer system (Fujifilm, Tokyo, Japan). The protein bands of GRP78 and β-actin were quantified by Multi Gauge software (Fujifilm), and the values of GRP78 expression were normalized with those of β-actin.

Quantitative reverse transcriptase PCR. HCV RNA was estimated by the method described previously (56). Total RNA was prepared from cells by using an RNeasy minikit (Qiagen, Tokyo, Japan). First-strand cDNA was synthesized using an RNA LA PCR in vitro cloning kit (Takara Bio Inc., Shiga, Japan) and random primers. Each cDNA was estimated with Platinum SYBR green qPCR SuperMix UDG (Invitrogen) according to the manufacturer's protocol. Fluorescent signals were analyzed with an ABI Prism 7000 (Applied Biosystems). The internal ribosomal entry site regions of HCV and mRNAs of GAPDH (glyceraldehyde-3-phosphate dehydrogenase), GRP78, and growth arrest- and DNA damage-inducible gene 153 (GADD153) were amplified using the primer pairs 5′-GAGTGTCGTGCAGCCTCCA-3′ and 5′-CACTCGCAAGCACCCTATCA-3′, 5′-GAAGGTGAAGGTCGGAGTC-3′ and 5′-GAAGGTGAAGGTCGGAGTC-3′, 5′-CGCCAAGCGGCTCATC-3′ and 5′-AACCACCTTGAACGGCAAGA-3′, and 5′-AGCTGGAACCTGAGGAGAGA-3′ and 5′-TGGATCAGTCTGGAAAAGCA-3′, respectively. The values of the HCV genome or each mRNA were normalized with those of GAPDH mRNA. Each PCR product was detected as a single band of the correct size on agarose gel electrophoresis (data not shown).

In vitro transcription and RNA transfection. The plasmid pFK-I_{389} neo/NS3-3′/NK5.1 was linearized by treatment with ScaI and then transcribed in vitro using the MEGAscript T7 kit (Applied Biosystems) according to the manufacturer's protocol. The in vitro-transcribed RNA was electroporated into cells at 4 million cells/0.4 ml under conditions of 270 V and 960 μF using a Gene Pulser (Bio-Rad, Hercules, CA). The colony formation assay was carried out by a method described previously (45).

Indirect immunofluorescence assay. Cells cultured on glass slides were fixed with 4% paraformaldehyde in phosphate-buffered saline (PBS) at room temperature for 30 min. After being washed twice with PBS, the cells were permeabilized for 20 min at room temperature with PBS containing 0.25% saponin and blocked with PBS containing 0.2% gelatin (gelatin-PBS) for 60 min at room temperature. The cells were incubated with gelatin-PBS containing rabbit anti-hB-ind1 antibody, mouse anti-NS5A IgG1, mouse anti-PDI IgG2a, mouse anti-FKBP8 IgG2b, or mouse anti-dsRNA IgG2a (J1 and K2) at 37°C for 60 min; washed three times with PBS containing 1% Tween 20; and incubated with gelatin-PBS containing AF488-conjugated anti-mouse IgG1 or AF647-conjugated anti-rabbit or AF594-conjugated anti-mouse IgG2a or IgG2b antibodies at 37°C for 60 min. Finally, the cells were washed three times with PBS containing 1% Tween 20 and observed with a FluoView FV1000 laser scanning confocal microscope (Olympus, Tokyo, Japan).

Correlative FM-EM. Correlative fluorescence microscopy-electron microscopy (FM-EM) allows individual cells to be examined both in an overview with FM and in a detailed subcellular-structure view with EM (51). The endogenous hB-ind1 and NS5A were stained and observed in the HCV replicon cells by the correlative FM-EM method as described previously (45).

Luciferase assay. Each plasmid was transfected into Huh7, Huh9-13, and interferon (IFN)-cured cells seeded in a 12-well plate, and the cells were treated with 1 μM dexamethasone (Sigma) for 12 h or with 17-dimethylamino-ethylamino-17-demethoxygeldanamycin (DMAG) (Sigma) for 6 h at 36 h posttransfection and lysed in 200 μl of passive lysis buffer (Promega). Luciferase activity was measured in 20-μl aliquots of the cell lysates using a Dual-Luciferase Reporter Assay System (Promega). Firefly luciferase activity was standardized with that of *Renilla* luciferase cotransfected with the internal-control plasmid pRL-TK. The resulting values were expressed as the increase in relative light units (RLU).

Statistical analysis. Results were expressed as the mean ± standard deviation. The significance of differences in the means was determined by Student's *t* test.

RESULTS

The p23-like domain of hB-ind1 has cochaperone activity. Although we had previously reported that hB-ind1 regulates HCV RNA replication through interaction with NS5A and Hsp90, the molecular mechanisms underlying the regulation of HCV replication remained to be clarified. To gain more insights into the potential cochaperone activity of hB-ind1 in the Hsp90 chaperone system, we prepared expression plasmids encoding a wild-type p23 and three p23 mutants—one in which the FXXW motif was replaced with AXXA (p23AxxA), one in which the cochaperone domain of p23 was replaced with the p23-like domain of hB-ind1 (cp23), and one in which both substitutions were made (cp23AxxA) (Fig. 1A). HA-tagged Hsp90 was coexpressed with FLAG-tagged p23 or the FLAG-tagged p23 mutants in 293T cells (Fig. 1B). Hsp90 was coimmunoprecipitated with wild-type p23 and a cp23 mutant, but not with the p23AxxA or cp23AxxA mutants, indicating that the FXXW motif of hB-ind1, as is the case with that of p23

Downloaded from jvi.asm.org at Osaka University on September 23, 2009

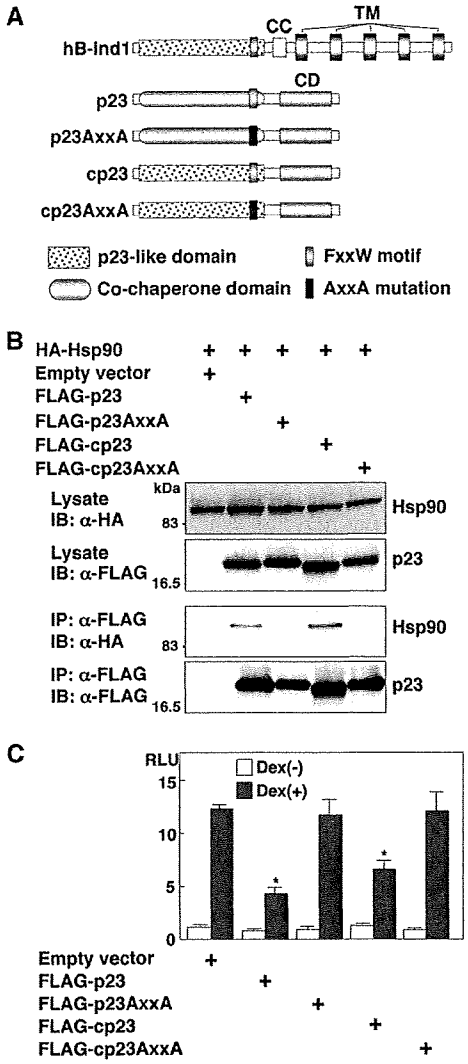

FIG. 1. Construction and characterization of p23 mutants. (A) Structures of hB-ind1, p23, and the three p23 mutants. hB-ind1 consists of a p23-like domain, an FXXW motif, a coiled-coil domain (CC), and a transmembrane domain (TM). p23 consists of a cochaperone domain, an FXXW motif, and a chaperone domain (CD). The three p23 mutants, p23AxxA, cp23, and cp23AxxA, were constructed by replacing the FXXW motif with AXXA, the cochaperone domain of p23 with the p23-like domain of hB-ind1, and both of the regions, respectively. (B) FLAG-tagged p23, p23AxxA, cp23, or cp23AxxA was coexpressed with HA-tagged Hsp90 in 293T cells and immunoprecipitated (IP) with anti-FLAG antibody. The immunoprecipitates were subjected to immunoblotting (IB). (C) The expression plasmid encoding FLAG-tagged p23, cp23, p23AxxA, or cp23AxxA was cotransfected with pGR-luc and pRL-TK plasmids into 293T cells and treated with 1 mM dexamethasone [Dex(+)] at 36 h posttransfection or untreated [Dex(−)], and the luciferase activities were determined at 12 h of incubation. The firefly luciferase activity was normalized with that of *Renilla* luciferase, and the GR-responsive promoter activity was indicated as the RLU. The error bars indicate standard deviations. The asterisks indicate significant differences ($P < 0.01$) versus the control value. The data shown are representative of three independent experiments.

(67), is also involved in binding to Hsp90. Hsp90 participates in the folding and stabilization of the ligand-binding domain of the glucocorticoid receptor (GR), together with p23 and other cofactors (49). p23 was shown to act not only in the activation (30), but also in the inhibition, of GR signaling (67). To examine whether hB-ind1 has the ability to work as a cochaperone in an Hsp90-dependent manner, each of the plasmids encoding p23 or the p23 mutants was cotransfected with a reporter plasmid carrying a firefly luciferase gene under the control of the GR promoter (pGR-luc), together with an internal-control plasmid (pRL-TK), and GR-mediated transcriptional activity was determined at 12 h after treatment with dexamethasone, a ligand of GR. Expression of the p23 or cp23 mutant, but not of the AXXA mutants, significantly inhibited GR-mediated transcription (Fig. 1C). These results indicate that the p23-like domain of hB-ind1 possesses cochaperone activity comparable to that of p23.

The p23-like domain of hB-ind1 is interchangeable with the p23 cochaperone domain during complex formation with NS5A, Hsp90, and FKBP8. Previous reports have suggested that HCV NS5A interacts with several host proteins, including FBL2 (63), vesicle-associated membrane protein-associated protein subtype A (VAP-A) (61), VAP-B (25), FKBP8 (45), and hB-ind1 (56), and that these interactions participate in the replication of HCV. We have shown that hB-ind1 interacts with NS5A and Hsp90 through the coiled-coil domain and the FXXW motif in the p23-like domain, respectively, and that coexpression of FKBP8 enhances the interaction of Hsp90 with hB-ind1 (56). To determine the effect of the mutation in the p23-like domain of hB-ind1 on interaction with Hsp90, NS5A, and FKBP8, we prepared an expression plasmid encoding wild-type hB-ind1 and three hB-ind1 mutants, one in which the p23-like domain was replaced with the cochaperone domain of p23 (chB-ind1), one in which the FXXW motif was replaced with AXXA (hB-ind1AxxA), and one in which both replacements were made (chB-ind1AxxA) (Fig. 2A). The FLAG-tagged wild-type or mutant hB-ind1 was coexpressed with HA-tagged Hsp90 (Fig. 2B, left) or HA-tagged NS5A (Fig. 2B, right) in 293T cells and immunoprecipitated with anti-FLAG antibody. Hsp90 was coprecipitated with wild-type hB-ind1 and the chB-ind1 mutant, but not with the hB-ind1AXXA and chB-ind1AXXA mutants (Fig. 2B, left), confirming that the FXXW motif is crucial for the interaction with Hsp90. In contrast, NS5A was coprecipitated with each of the hB-ind1 proteins, suggesting that mutation in the p23-like domain of hB-ind1 has no effect on the binding of hB-ind1 to NS5A through the coiled-coil domain (Fig. 2B, right). To determine the effect of FKBP8 expression on the interaction between hB-ind1 and Hsp90, FLAG-tagged wild-type hB-ind1 or the chB-ind1 mutant was coexpressed with HA-tagged FKBP8 and/or Hsp90 in 293T cells and immunoprecipitated with anti-FLAG antibody. The amounts of Hsp90 coprecipitated with hB-ind1 or chB-ind1 were increased by coexpression of FKBP8 (Fig. 2C). To further examine the interaction of hB-ind1 with Hsp90 and NS5A at an endogenous expression level in Huh9-13 cells harboring an HCV subgenomic RNA replicon, lysates of the replicon cells were subjected to immunoprecipitation analysis. Endogenous Hsp90 and NS5A were specifically coimmunoprecipitated with endogenous hB-ind1 (Fig. 2D). These results suggest that the p23-like domain of hB-ind1 is inter-

Downloaded from jvi.asm.org at Osaka University on September 23, 2009

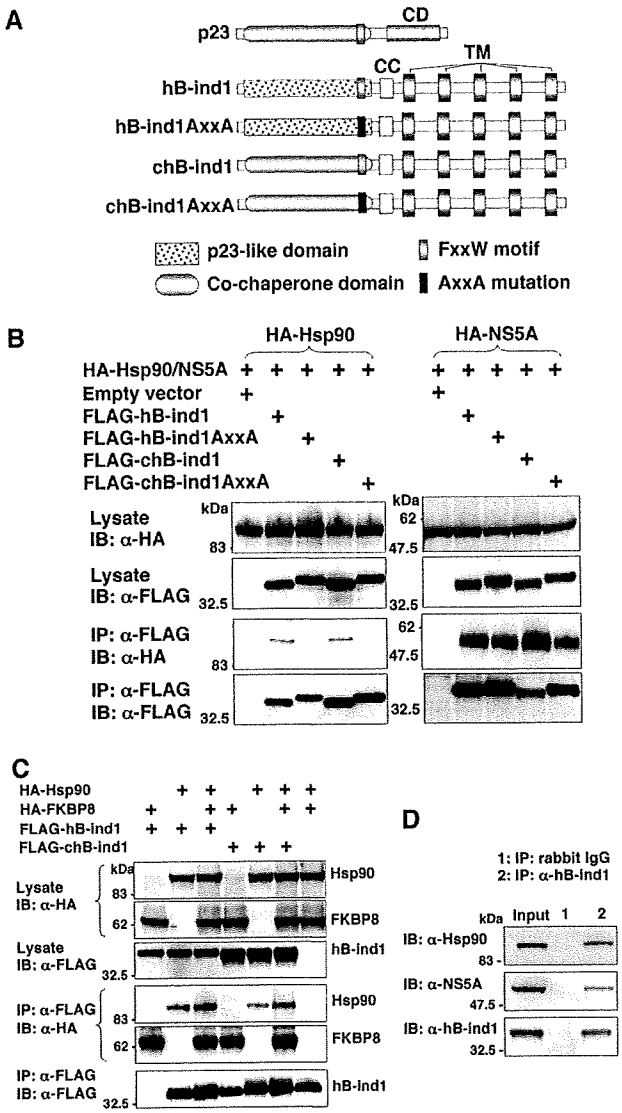

FIG. 2. Construction and characterization of hB-ind1 mutants. (A) Structures of p23, hB-ind1, and the three hB-ind1 mutants. The three hB-ind1 mutants, hB-ind1AxxA, chB-ind1, and chB-ind1AxxA, were constructed by replacing the FXXW motif with AXXA, the p23-like domain of hB-ind1 with the cochaperone domain of p23, and both of the regions, respectively. (B) FLAG-tagged hB-ind1, hB-ind1 AxxA, chB-ind1, or chB-ind1AxxA was coexpressed with either HA-tagged Hsp90 (left) or NS5A (right) in 293T cells and immunoprecipitated (IP) with anti-FLAG antibody. The immunoprecipitates were subjected to immunoblotting (IB). (C) HA-tagged Hsp90 and HA-FKBP8 were expressed with FLAG-tagged hB-ind1 and chB-ind1 in various combinations in 293T cells and immunoprecipitated with anti-FLAG antibody, and the immunoprecipitates were detected by immunoblotting. (D) Endogenous hB-ind1 in Huh9-13 cells harboring subgenomic HCV replicon RNA was immunoprecipitated with anti-hB-ind1 rabbit IgG (lane 2). The cell lysate was mixed with normal rabbit IgG as a negative control (lane 1). The immunoprecipitates were analyzed by immunoblotting with an antibody to Hsp90, NS5A, or hB-ind1. The data shown are representative of three independent experiments.

changeable with the cochaperone domain of p23 during complex formation with NS5A, Hsp90, and FKBP8.

Cochaperone activity in the p23-like domain of hB-ind1 is required for propagation of HCV. The p23-like domain of hB-ind1 has been suggested to be required for HCV propagation (56). However, the involvement of the cochaperone activity of hB-ind1 in HCV propagation has not been examined. To assess the effect of cochaperone activity in the p23-like domain of hB-ind1 on the RNA replication and particle production of HCV, each of the expression plasmids encoding the FLAG-tagged wild-type or mutant hB-ind1 carrying the silent mutations resistant to small interfering RNA was transfected into hB-ind1 knockdown (Huh-KD) cells and cultured for a week in the presence of puromycin. The expressions of FLAG-tagged hB-ind1 and the mutants in the Huh-KD cells were comparable to that of the endogenous hB-ind1 in the control (Huh-ctrl) cells transfected with an empty vector (Fig. 3A). Subgenomic HCV replicon RNA transcribed from pFK-I_{389} neo/NS3-3′/NK5.1 was transfected into these cells and cultured for 4 weeks in the presence of G418. Although the number of colonies was reduced in the Huh-KD cells compared with the Huh-ctrl cells after transfection with an empty vector, as described previously (56), the colony numbers were recovered by the expression of the hB-ind1 or chB-ind1 mutant, but not by that of the hB-ind1AXXA or chB-ind1AXXA mutants (Fig. 3B). Similarly, intracellular HCV RNA and infectious viral titers in the culture supernatants of Huh-KD cells infected with JFH1 virus were partially recovered by the expression of the hB-ind1 or chB-ind1 mutant, but not by that of the hB-ind1AXXA or chB-ind1AXXA mutant (Fig. 3C). These results suggest that cochaperone activity in the p23-like domain of hB-ind1 is required for HCV propagation and that the cochaperone domain of p23 can substitute for the p23-like domain of hB-ind1.

hB-ind1 colocalizes with NS5A, FKBP8, and dsRNA on the membranous web. Our previous report revealed the interplay among hB-ind1, Hsp90, FKBP8, and NS5A and showed that these interactions play an important role in HCV replication (56). However, the subcellular localization of the endogenous hB-ind1 in the replicon cells and JFH1 virus-infected cells has not been precisely assessed. To determine the subcellular localization of hB-ind1 in the context of HCV replication, the expression of hB-ind1 and NS5A in the replicon cells and JFH1 virus-infected cells was examined by immunofluorescence analyses (Fig. 4A). Endogenous hB-ind1 was colocalized with the endoplasmic reticulum (ER)-marker PDI and NS5A as dot-like structures in the Huh9-13 replicon cells (Fig. 4A, top) and in cells infected with JFH1 virus (Fig. 4A, bottom), and these dot-like structures disappeared in concert with the loss of NS5A expression by treatment with IFN-α in the replicon cells and was not observed in the mock-infected Huh7.5.1 cells. Furthermore, FKBP8 (Fig. 4B, top) and dsRNA (Fig. 4B, bottom) were colocalized with hB-ind1 and NS5A in the dot-like structures in Huh9-13 replicon cells. These results indicate that HCV replicating RNA is localized with hB-ind1, FKBP8, and NS5A in the dot-like compartments. HCV RNA replication or expression of viral proteins leads to formation of the convoluted membranous structures designated the membranous web (14, 23). The large structures of the replication complexes in the replicon cells indicate membranous webs with

Downloaded from jvi.asm.org at Osaka University on September 23, 2009

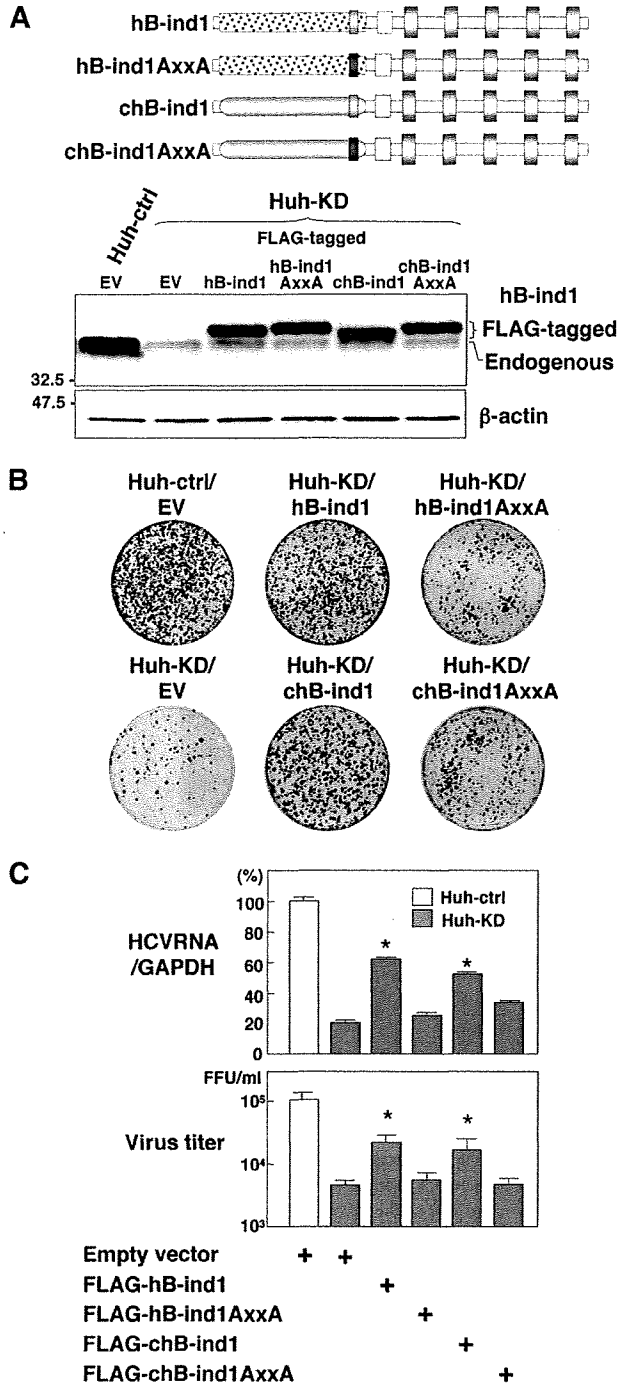

FIG. 3. Effects of the cochaperone activity of hB-ind1 on the propagation of HCV. (A) Huh-KD cells were transfected with either an empty vector or an expression plasmid encoding FLAG-tagged hB-ind1, hB-ind1AxxA, chB-ind1, or chB-ind1AxxA, which are resistant to small interfering RNA due to the introduction of silent mutations, and cultured for a week in the presence of 10 μg/ml of puromycin. The surviving cells were used in the subsequent experiments. The endogenous and exogenous expression of hB-ind1 and the mutants was detected by immunoblotting. The control cell line (Huh-ctrl) or the Huh-KD cell line transfected with an empty vector (EV) was used as a control. (B) Huh-KD cells were transfected with the plasmids and then selected with puromycin. The resulting cells were further transfected with a replicon RNA transcribed from pFK-I_{389} neo/NS3-3'/NK5.1, cultured for 4 weeks in the presence of 1 mg/ml of G418, and stained with crystal violet after fixation with 4% paraformaldehyde. The Huh-KD cell line transfected with an empty vector (EV) was used as a positive control. (C) The cells prepared as described above were infected with JFH1 virus and harvested at 3 days postinfection. The amount of intracellular HCV RNA was estimated by quantitative reverse transcriptase PCR and normalized with that of GAPDH mRNA. The values of HCV RNA are presented as percentages versus those of Huh-ctrl cells transfected with an empty vector. The culture supernatants were subjected to a focus-forming assay. Virus titers are presented as focus-forming units (FFU) per ml. The error bars indicate standard deviations. The asterisks indicate significant differences ($P < 0.01$) versus the value of the control. The data shown are representative of three independent experiments.

restricted motility (68). To further analyze the subcellular compartments, including hB-ind1 and NS5A, the same field of the Huh9-13 replicon cells was observed under FM and EM by using the correlative FM-EM technique (Fig. 5A, upper two rows). The large structures that included hB-ind1 and NS5A in the replicon cells were observed under FM and EM (white-boxed areas) and further magnified (black-boxed areas). Convoluted membranous structures that consisted of small vesicles and that were similar to the membranous web were observed. Another field of view yielded similar results (Fig. 5A, lower two rows). The membranous web resembling the convoluted structures was not observed in the Huh9-13 cells depleted of viral RNA by IFN treatment (Fig. 5B). Together, these results suggest that hB-ind1 interacts with NS5A on the membranous web in cells replicating HCV RNA.

Hsp90 is involved in the circumvention of the UPR during HCV replication. Hsp90 regulates the folding and stability of proteins in all eukaryotes (59), and inhibition of the chaperone pathway suppresses correct protein folding, which leads to induction of proteasome-mediated degradation of the unfolded proteins and the unfolded protein response (UPR). Our previous (46) and present studies (Fig. 4 and 5) showed that several cochaperone components are recruited in the membranous web, suggesting that the Hsp90 chaperone system participates in the replication complex to circumvent the induction of the UPR and to maintain the folding of the host and viral proteins in a replication-competent state. To determine the induction of the UPR by HCV replication, Huh9-13 replicon cells were transfected with a reporter plasmid carrying a firefly luciferase gene under the control of the GRP78 promoter, which is activated by the induction of the UPR, together with an internal-control plasmid. Although the GRP78 promoter activity was slightly enhanced in the Huh9-13 cells compared to that in the parental cells, a fourfold increase of GRP78 promoter activity in the replicon cells was observed after treatment with an Hsp90 inhibitor, DMAG, in contrast to the twofold increase in similarly treated parental Huh7 cells, and the activation of the GRP78 promoter was canceled by treatment with IFN-α despite DMAG treatment (Fig. 6A), suggesting that the Hsp90 chaperone system participates in the circumvention of the UPR induced by the replication of HCV RNA. In addition, activation of GRP78 at transcriptional and translational levels after treatment with DMAG was higher in the

Downloaded from jvi.asm.org at Osaka University on September 23, 2009

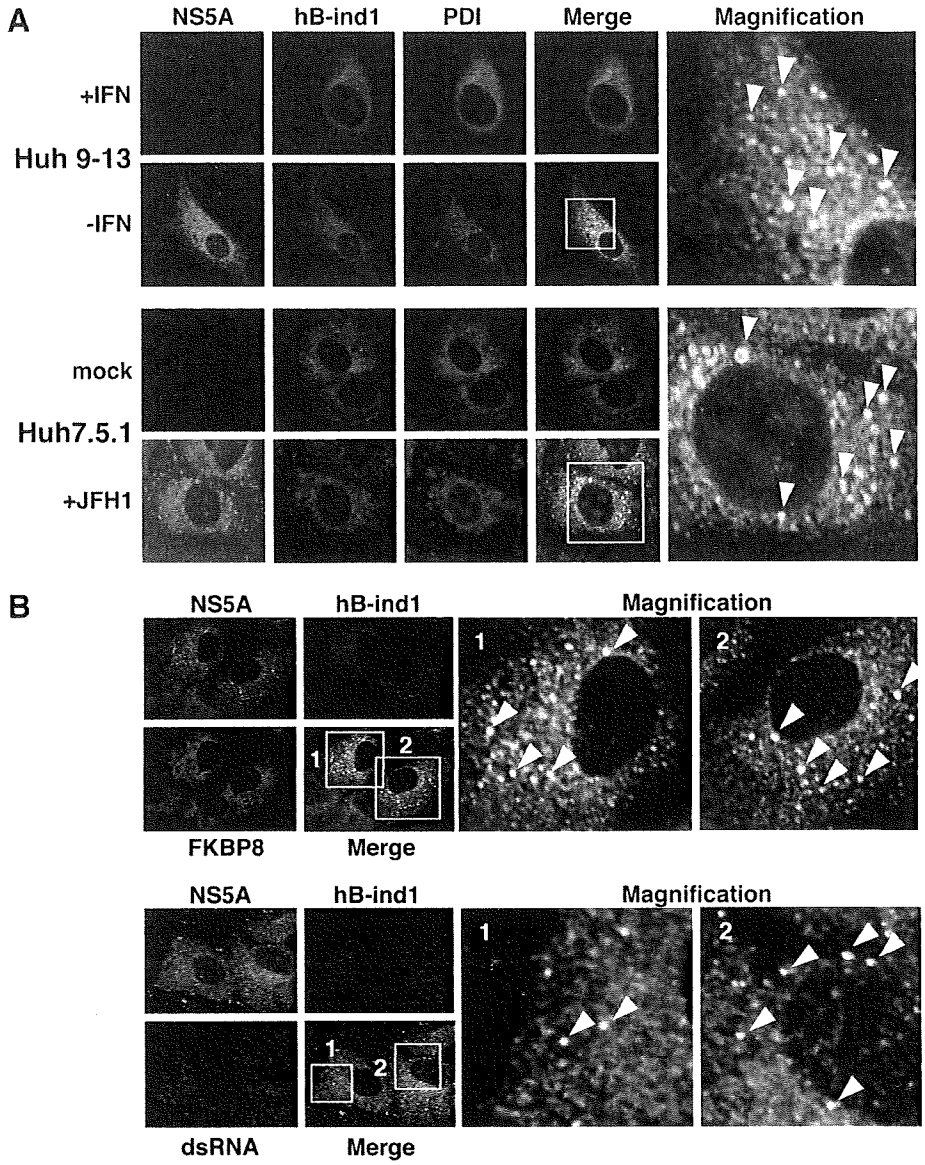

FIG. 4. Intracellular localization of hB-ind1 in replicon cells and infected cells. (A) Huh9-13 replicon cells with IFN-α or untreated and Huh7.5.1 cells infected with JFH1 virus or naïve cells were stained with antibodies against NS5A, hB-ind1, or PDI and examined by immunofluorescence assay. The boxed areas in the merged images are magnified and displayed on the right. The arrowheads indicate intracellular positions colocalized with NS5A, hB-ind1, and PDI. (B) Huh9-13 replicon cells were fixed, permeabilized, and stained with appropriate antibodies to NS5A, hB-ind1, and FKBP8 (top) or dsRNA (bottom). The boxed areas in the merged images are magnified and displayed on the right. The arrowheads indicate intracellular positions colocalized with NS5A, hB-ind, and FKBP8 or dsRNA. The images shown are representative of three independent experiments.

HCV replicon cells than in the parental cells or in cured cells, which were depleted of HCV RNA by treatment with IFN-α (Fig. 6B). Furthermore, DMAG treatment enhanced the transcription of the UPR marker protein GADD153 at a higher level in the replicon cells than in the parental Huh7 or the cured cells (Fig. 6C). These results suggest that the Hsp90-dependent chaperone system plays a crucial role in the folding of the host and viral proteins involved in HCV replication and in the regulation of UPR induction.

DISCUSSION

Studies of the relationship between Hsp90 and steroid receptors, such as GR, have revealed the activities of cochaperones (52, 67). Cochaperones, such as p23, appear to interact with and dissociate from Hsp90 and the client protein complex in a defined order. These cochaperones participate in the chaperone complex in a late step and promote the dissociation of the client proteins from Hsp90 to facilitate formation of the

Downloaded from jvi.asm.org at Osaka University on September 23, 2009

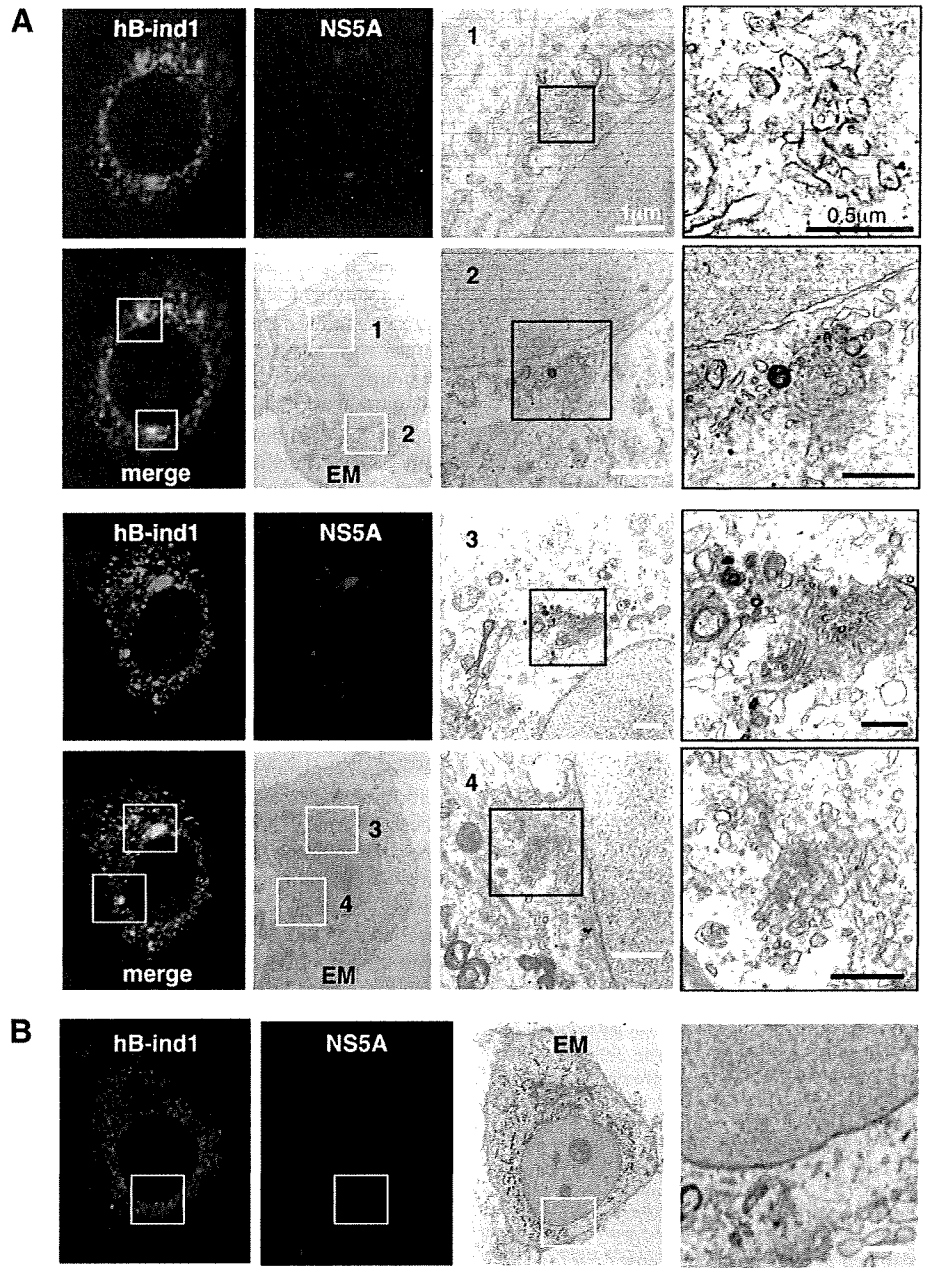

FIG. 5. hB-ind1 interacts with NS5A in the membranous web. Huh9-13 replicon cells were stained with specific antibodies to hB-ind1 and NS5A. Identical fields of Huh9-13 (A) or the cured cells (B) were observed under EM by using the correlative FM-EM technique. The white-boxed areas indicate the colocalized areas of hB-ind1 with NS5A. Magnified views of the white-boxed areas are displayed in the third column from the left. The right column contains further-magnified images of each of the black-boxed areas. Another field of view is presented in the lower two rows.

chaperone complex in the next chaperone cycle (16–18). In this study, we have shown that hB-ind1 participates in HCV replication and that the p23-like domain of hB-ind1 possesses cochaperone activity comparable to that of the cochaperone domain of p23, suggesting that hB-ind1 is involved in the recycling of the chaperone complex in the membranous web to maintain the function of the replication complex of HCV.

Previous studies have indicated that HCV proteins rearrange the ER membrane into the small convoluted membranous vesicles that are collectively known as the membranous web, and these vesicles have been suggested to be the intracellular compartments in which HCV replication takes place (14, 23, 68). In the living replicon cells, two forms of replication complexes, small and large vesicles, are detected, both of which include the viral replication complexes (68). Large vesicles, corresponding to membranous webs, exhibit restricted motil-

Downloaded from jvi.asm.org at Osaka University on September 23, 2009

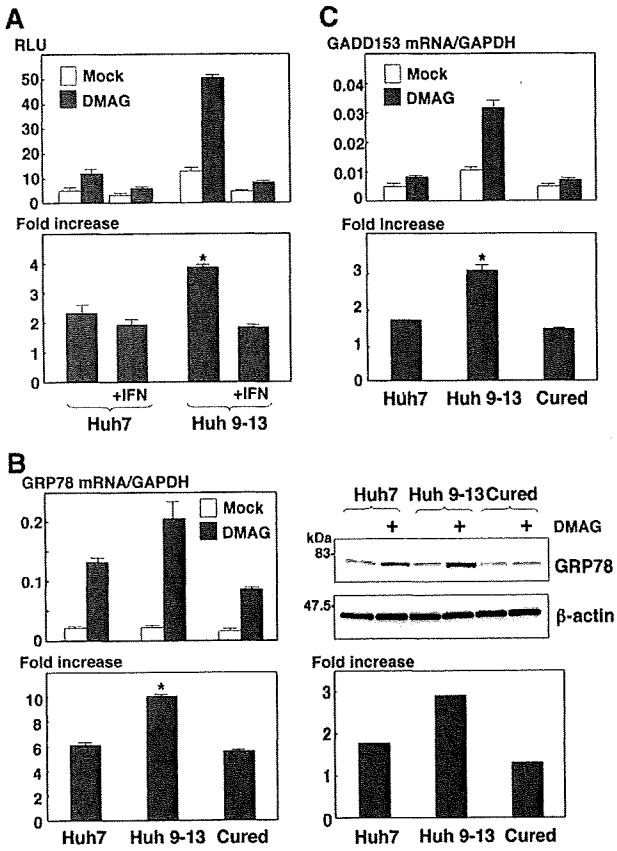

FIG. 6. Effect of Hsp90 inhibitor on the induction of the UPR in HCV replicon cells. (A) Huh7 and Huh9-13 replicon cells were transfected with a reporter plasmid, pGRP78-luc, and an internal-control plasmid, pRL-TK. The transfected cells were treated with IFN-α (+IFN) from 6 to 36 h posttransfection or left untreated and then further incubated for 6 h in the presence or absence of 1 μM DMAG. The resulting cells were harvested and subjected to a dual-luciferase assay. The firefly luciferase activity is indicated as the RLU (top) after standardization with that of *Renilla* luciferase. The enhancement of promoter activity by treatment with DMAG is presented as the increase (bottom). (B) Huh7 cells, Huh9-13 cells, and Huh9-13 cells cured by IFN-α treatment (Cured) were cultured for 6 h in the presence or absence of 1 μM DMAG, and the amount of GRP78 mRNA was measured by real-time PCR. The value of the mRNA was normalized with the amount of GAPDH mRNA (upper left), and the transcriptional enhancement by treatment with DMAG is presented as the increase (lower left). The expression levels of GRP78 and β-actin in the cells were determined by immunoblotting (upper right) and are presented as the increase (lower right). (C) The amounts of GADD153 mRNA in Huh7 cells, Huh9-13 cells, and the cured cells cultured for 6 h in the presence or absence of 1 μM DMAG were measured by real-time PCR. The values of the mRNA were normalized with the amount of GAPDH mRNA (top), and the transcriptional enhancement by treatment with DMAG is presented as the increase (bottom). The error bars indicate standard deviations. The asterisks indicate significant differences ($P < 0.01$) versus the control value. The data shown are representative of three independent experiments.

ity, while small vesicles show fast movement (68), and FM and EM have revealed that NS5A is colocalized with hB-ind1, as well as FKBP8 (45), in the membranous webs. hB-ind1 was first identified as a regulator of Rac1 that activates JNK and NF-κB (11). Rac1 is a member of the Rho GTPase family and plays crucial roles in cytoskeletal dynamics, membrane ruffling, and gene transcription through the effectors of the Rho GTPase family members. IQGAP1 and PAK1 are Rac1 effectors that bind to Rac proteins and are also involved in the replication of HCV (5, 7, 19, 31, 50). The tetratricopeptide repeat domain of immunophilin family members, such as FKBP8, has been shown to interact with Hsp90 (12, 45) and the GR-Hsp90 complex that leads to association with dynein for retrograde transport, along with microtubules (12). Hsp90 has been shown to play an important role in the interaction of transcriptase with genomic RNA of hepatitis B virus (27) and the nuclear transportation of the polymerase of influenza virus (40). Flock house virus also recruits Hsp90 in the polymerase synthesis in the early step of infection (9). Hsp90 may be involved in the regulation of the movement and arrangement of the HCV replication complexes through interaction with Rac1, hB-ind1, and FKBP8. Further investigation is needed to clarify the role of the Hsp90 chaperone system in the life cycle of HCV.

The surrounding membranes, including the membranous web, may protect the viral replication complex and RNA genome against digestion by the host proteases and nucleases (69). The replication complex is composed of viral nonstructural proteins and host proteins, including chaperone and cochaperone proteins. HCV NS5A has been shown to interact with various host proteins, including cochaperones, such as FKBP8 and hB-ind1, and to recruit a chaperone, Hsp90, into the replication complex through interaction with these cochaperones. Recruitment of the chaperone complex into the replication complex is crucial for the correct folding of newly synthesized viral proteins to maintain the efficient replication of the viral genome. HCV replication has been shown to be improved by the adaptive mutations suppressing the phosphorylation status of NS5A in the replicon cells (3). Although suppression of the hyperphosphorylation of NS5A by treatment with kinase inhibitors improves the replication of the replicons that have no adaptive mutations (42), several kinase inhibitors have been shown to suppress the replication of the HCV replicon carrying the adaptive mutations (29), and phosphorylation of NS5A by casein kinase II was shown to improve virus production but not HCV RNA replication (57). Hsp90 is capable of directly modulating the activities of several kinases (37, 53, 54), and thus, it might be feasible that cochaperones, including hB-ind1 and FKBP8, participate in the propagation of HCV by regulating the phosphorylation status of NS5A in cooperation with Hsp90.

The host chaperone system regulates the quality of client proteins, and impairment of the chaperone activity induces accumulation of misfolded proteins and affects the natural cellular function and viability (20, 21, 33). In this study, DMAG treatment induced a higher level of UPR in HCV replicon cells than in parental and cured cells, indicating that the Hsp90 chaperone system participates in the maintenance of correct folding of the viral and host proteins in the replication complex in the membranous web and in the circumvention of the UPR induced by HCV replication. Treatment with geldanamycin or its derivatives has been shown to inhibit GRP94, which is the Hsp90 paralog located in the ER (10), and to disrupt the ER chaperone pathway, leading to the induction of ER-associated protein degradation, transcriptional attenuation, and eventually induction of apoptosis (34). ER chaperones, such as

Downloaded from jvi.asm.org at Osaka University on September 23, 2009

GRP94, may also participate in the correct folding of the viral and host proteins in the replication complex for efficient replication of the HCV genome.

Geldanamycin and its derivatives have been reported to remarkably inhibit poliovirus replication in vivo without any emergence of drug-resistant escape mutants (22), suggesting that an inhibitor of the chaperone system may be a promising candidate for the treatment of viral infectious diseases with low risk of the emergence of drug-resistant viruses. In addition, Hsp90 inhibitors exhibit anticancer activities through the suppression of various cell signals essential for cancer growth and the enhancement of radiation sensitivity (2, 8, 13). In conclusion, our data indicate that hB-ind1 is included within the HCV replication complex and regulates HCV RNA replication through its own cochaperone activity. Hsp90 and cochaperones, including hB-ind1 and FKBP8, which are required for efficient HCV replication, should be ideal targets for the treatment of chronic hepatitis C with a low frequency of emergence of drug-resistant breakthrough viruses.

ACKNOWLEDGMENTS

We thank H. Murase for her secretarial work. We also thank R. Bartenschlager, T. Wakita, and F. V. Chisari for providing the plasmids and cell lines.

This work was supported in part by grants-in-aid from the Ministry of Health, Labor, and Welfare; the Ministry of Education, Culture, Sports, Science, and Technology; the Global Center of Excellence Program; the Foundation for Biomedical Research and Innovation; and the Naito Foundation.

REFERENCES

1. **Abe, T., Y. Kaname, I. Hamamoto, Y. Tsuda, X. Wen, S. Taguwa, K. Moriishi, O. Takeuchi, T. Kawai, T. Kanto, N. Hayashi, S. Akira, and Y. Matsuura.** 2007. Hepatitis C virus nonstructural protein 5A modulates the toll-like receptor-MyD88-dependent signaling pathway in macrophage cell lines. J. Virol. **81**:8953–8966.
2. **Bisht, K. S., C. M. Bradbury, D. Mattson, A. Kaushal, A. Sowers, S. Markovina, K. L. Ortiz, L. K. Sieck, J. S. Isaacs, M. W. Brechbiel, J. B. Mitchell, L. M. Neckers, and D. Gius.** 2003. Geldanamycin and 17-allylamino-17-demethoxygeldanamycin potentiate the in vitro and in vivo radiation response of cervical tumor cells via the heat shock protein 90-mediated intracellular signaling and cytotoxicity. Cancer Res. **63**:8984–8995.
3. **Blight, K. J., A. A. Kolykhalov, and C. M. Rice.** 2000. Efficient initiation of HCV RNA replication in cell culture. Science **290**:1972–1974.
4. **Bohen, S. P., A. Kralli, and K. R. Yamamoto.** 1995. Hold 'em and fold 'em: chaperones and signal transduction. Science **268**:1303–1304.
5. **Bost, A. G., D. Venable, L. Liu, and B. A. Heinz.** 2003. Cytoskeletal requirements for hepatitis C virus (HCV) RNA synthesis in the HCV replicon cell culture system. J. Virol. **77**:4401–4408.
6. **Brown, G., H. W. Rixon, J. Steel, T. P. McDonald, A. R. Pitt, S. Graham, and R. J. Sugrue.** 2005. Evidence for an association between heat shock protein 70 and the respiratory syncytial virus polymerase complex within lipid-raft membranes during virus infection. Virology **338**:69–80.
7. **Bryan, B. A., D. Li, X. Wu, and M. Liu.** 2005. The Rho family of small GTPases: crucial regulators of skeletal myogenesis. Cell Mol. Life Sci. **62**: 1547–1555.
8. **Calderwood, S. K., M. A. Khaleque, D. B. Sawyer, and D. R. Ciocca.** 2006. Heat shock proteins in cancer: chaperones of tumorigenesis. Trends Biochem. Sci. **31**:164–172.
9. **Castorena, K. M., S. A. Weeks, K. A. Stapleford, A. M. Cadwallader, and D. J. Miller.** 2007. A functional heat shock protein 90 chaperone is essential for efficient flock house virus RNA polymerase synthesis in *Drosophila* cells. J. Virol. **81**:8412–8420.
10. **Chavany, C., E. Mimnaugh, P. Miller, R. Bitton, P. Nguyen, J. Trepel, L. Whitesell, R. Schnur, J. Moyer, and L. Neckers.** 1996. p185erbB2 binds to GRP94 in vivo. Dissociation of the p185erbB2/GRP94 heterocomplex by benzoquinone ansamycins precedes depletion of p185erbB2. J. Biol. Chem. **271**:4974–4977.
11. **Courilleau, D., E. Chastre, M. Sabbah, G. Redeuilh, A. Atfi, and J. Mester.** 2000. B-ind1, a novel mediator of Rac1 signaling cloned from sodium butyrate-treated fibroblasts. J. Biol. Chem. **275**:17344–17348.
12. **Davies, T. H., Y. M. Ning, and E. R. Sanchez.** 2002. A new first step in activation of steroid receptors: hormone-induced switching of FKBP51 and FKBP52 immunophilins. J. Biol. Chem. **277**:4597–4600.
13. **Didelot, C., D. Lanneau, M. Brunet, A. L. Joly, A. De Thonel, G. Chiosis, and C. Garrido.** 2007. Anti-cancer therapeutic approaches based on intracellular and extracellular heat shock proteins. Curr. Med. Chem. **14**:2839–2847.
14. **Egger, D., B. Wolk, R. Gosert, L. Bianchi, H. E. Blum, D. Moradpour, and K. Bienz.** 2002. Expression of hepatitis C virus proteins induces distinct membrane alterations including a candidate viral replication complex. J. Virol. **76**:5974–5984.
15. **Evans, M. J., C. M. Rice, and S. P. Goff.** 2004. Genetic interactions between hepatitis C virus replicons. J. Virol. **78**:12085–12089.
16. **Freeman, B. C., S. J. Felts, D. O. Toft, and K. R. Yamamoto.** 2000. The p23 molecular chaperones act at a late step in intracellular receptor action to differentially affect ligand efficacies. Genes Dev. **14**:422–434.
17. **Freeman, B. C., and K. R. Yamamoto.** 2002. Disassembly of transcriptional regulatory complexes by molecular chaperones. Science **296**:2232–2235.
18. **Frydman, J., and J. Hohfeld.** 1997. Chaperones get in touch: the Hip-Hop connection. Trends Biochem. Sci. **22**:87–92.
19. **Fukata, M., M. Nakagawa, and K. Kaibuchi.** 2003. Roles of Rho-family GTPases in cell polarisation and directional migration. Curr. Opin. Cell Biol. **15**:590–597.
20. **Garrido, C., M. Brunet, C. Didelot, Y. Zermati, E. Schmitt, and G. Kroemer.** 2006. Heat shock proteins 27 and 70: anti-apoptotic proteins with tumorigenic properties. Cell Cycle **5**:2592–2601.
21. **Garrido, C., S. Gurbuxani, L. Ravagnan, and G. Kroemer.** 2001. Heat shock proteins: endogenous modulators of apoptotic cell death. Biochem. Biophys. Res. Commun. **286**:433–442.
22. **Geller, R., M. Vignuzzi, R. Andino, and J. Frydman.** 2007. Evolutionary constraints on chaperone-mediated folding provide an antiviral approach refractory to development of drug resistance. Genes Dev. **21**:195–205.
23. **Gosert, R., D. Egger, V. Lohmann, R. Bartenschlager, H. E. Blum, K. Bienz, and D. Moradpour.** 2003. Identification of the hepatitis C virus RNA replication complex in Huh-7 cells harboring subgenomic replicons. J. Virol. **77**:5487–5492.
24. **Grakoui, A., D. W. McCourt, C. Wychowski, S. M. Feinstone, and C. M. Rice.** 1993. Characterization of the hepatitis C virus-encoded serine proteinase: determination of proteinase-dependent polyprotein cleavage sites. J. Virol. **67**:2832–2843.
25. **Hamamoto, I., Y. Nishimura, T. Okamoto, H. Aizaki, M. Liu, Y. Mori, T. Abe, T. Suzuki, M. M. Lai, T. Miyamura, K. Moriishi, and Y. Matsuura.** 2005. Human VAP-B is involved in hepatitis C virus replication through interaction with NS5A and NS5B. J. Virol. **79**:13473–13482.
26. **Ho, S. N., H. D. Hunt, R. M. Horton, J. K. Pullen, and L. R. Pease.** 1989. Site-directed mutagenesis by overlap extension using the polymerase chain reaction. Gene **77**:51–59.
27. **Hu, J., D. Flores, D. Toft, X. Wang, and D. Nguyen.** 2004. Requirement of heat shock protein 90 for human hepatitis B virus reverse transcriptase function. J. Virol. **78**:13122–13131.
28. **Huang, D. C., S. Cory, and A. Strasser.** 1997. Bcl-2, Bcl-XL and adenovirus protein E1B19kD are functionally equivalent in their ability to inhibit cell death. Oncogene **14**:405–414.
29. **Huang, Y., K. Staschke, R. De Francesco, and S. L. Tan.** 2007. Phosphorylation of hepatitis C virus NS5A nonstructural protein: a new paradigm for phosphorylation-dependent viral RNA replication? Virology **364**:1–9.
30. **Hutchison, K. A., L. F. Stancato, J. K. Owens-Grillo, J. L. Johnson, P. Krishna, D. O. Toft, and W. B. Pratt.** 1995. The 23-kDa acidic protein in reticulocyte lysate is the weakly bound component of the hsp foldosome that is required for assembly of the glucocorticoid receptor into a functional heterocomplex with hsp90. J. Biol. Chem. **270**:18841–18847.
31. **Ishida, H., K. Li, M. Yi, and S. M. Lemon.** 2007. p21-activated kinase 1 is activated through the mammalian target of rapamycin/p70 S6 kinase pathway and regulates the replication of hepatitis C virus in human hepatoma cells. J. Biol. Chem. **282**:11836–11848.
32. **Kampmueller, K. M., and D. J. Miller.** 2005. The cellular chaperone heat shock protein 90 facilitates Flock House virus RNA replication in *Drosophila* cells. J. Virol. **79**:6827–6837.
33. **Kim, H. P., D. Morse, and A. M. Choi.** 2006. Heat-shock proteins: new keys to the development of cytoprotective therapies. Exp. Opin. Ther. Targets **10**:759–769.
34. **Lai, E., T. Teodoro, and A. Volchuk.** 2007. Endoplasmic reticulum stress: signaling the unfolded protein response. Physiology **22**:193–201.
35. **Lohmann, V., F. Korner, J. Koch, U. Herian, L. Theilmann, and R. Bartenschlager.** 1999. Replication of subgenomic hepatitis C virus RNAs in a hepatoma cell line. Science **285**:110–113.
36. **McLauchlan, J., M. K. Lemberg, G. Hope, and B. Martoglio.** 2002. Intramembrane proteolysis promotes trafficking of hepatitis C virus core protein to lipid droplets. EMBO J. **21**:3980–3988.
37. **Miyata, Y., and I. Yahara.** 1992. The 90-kDa heat shock protein, HSP90, binds and protects casein kinase II from self-aggregation and enhances its kinase activity. J. Biol. Chem. **267**:7042–7047.
38. **Momose, F., T. Naito, K. Yano, S. Sugimoto, Y. Morikawa, and K. Nagata.**

Downloaded from jvi.asm.org at Osaka University on September 23, 2009

2002. Identification of Hsp90 as a stimulatory host factor involved in influenza virus RNA synthesis. J. Biol. Chem. **277**:45306–45314.
39. **Moradpour, D., F. Penin, and C. M. Rice.** 2007. Replication of hepatitis C virus. Nat. Rev. Microbiol. **5**:453–463.
40. **Naito, T., F. Momose, A. Kawaguchi, and K. Nagata.** 2007. Involvement of Hsp90 in assembly and nuclear import of influenza virus RNA polymerase subunits. J. Virol. **81**:1339–1349.
41. **Neckers, L.** 2002. Hsp90 inhibitors as novel cancer chemotherapeutic agents. Trends Mol. Med. **8**:S55–S61.
42. **Neddermann, P., M. Quintavalle, C. Di Pietro, A. Clementi, M. Cerretani, S. Altamura, L. Bartholomew, and R. De Francesco.** 2004. Reduction of hepatitis C virus NS5A hyperphosphorylation by selective inhibition of cellular kinases activates viral RNA replication in cell culture. J. Virol. **78**:13306–13314.
43. **Okamoto, K., Y. Mori, Y. Komoda, T. Okamoto, M. Okochi, M. Takeda, T. Suzuki, K. Moriishi, and Y. Matsuura.** 2008. Intramembrane processing by signal peptide peptidase regulates the membrane localization of hepatitis C virus core protein and viral propagation. J. Virol. **82**:8349–8361.
44. **Okamoto, K., K. Moriishi, T. Miyamura, and Y. Matsuura.** 2004. Intramembrane proteolysis and endoplasmic reticulum retention of hepatitis C virus core protein. J. Virol. **78**:6370–6380.
45. **Okamoto, T., Y. Nishimura, T. Ichimura, K. Suzuki, T. Miyamura, T. Suzuki, K. Moriishi, and Y. Matsuura.** 2006. Hepatitis C virus RNA replication is regulated by FKBP8 and Hsp90. EMBO J. **25**:5015–5025.
46. **Okamoto, T., H. Omori, Y. Kaname, T. Abe, Y. Nishimura, T. Suzuki, T. Miyamura, T. Yoshimori, K. Moriishi, and Y. Matsuura.** 2008. A single-amino-acid mutation in hepatitis C virus NS5A disrupting FKBP8 interaction impairs viral replication. J. Virol. **82**:3480–3489.
47. **Pietschmann, T., V. Lohmann, A. Kaul, N. Krieger, G. Rinck, G. Rutter, D. Strand, and R. Bartenschlager.** 2002. Persistent and transient replication of full-length hepatitis C virus genomes in cell culture. J. Virol. **76**:4008–4021.
48. **Prapapanich, V., S. Chen, E. J. Toran, R. A. Rimerman, and D. F. Smith.** 1996. Mutational analysis of the hsp70-interacting protein Hip. Mol. Cell. Biol. **16**:6200–6207.
49. **Pratt, W. B., and D. O. Toft.** 1997. Steroid receptor interactions with heat shock protein and immunophilin chaperones. Endocr. Rev. **18**:306–360.
50. **Ridley, A. J., H. F. Paterson, C. L. Johnston, D. Diekmann, and A. Hall.** 1992. The small GTP-binding protein rac regulates growth factor-induced membrane ruffling. Cell **70**:401–410.
51. **Rieder, C. L., and S. S. Bowser.** 1985. Correlative immunofluorescence and electron microscopy on the same section of epon-embedded material. J. Histochem. Cytochem. **33**:165–171.
52. **Sanchez, E. R., D. O. Toft, M. J. Schlesinger, and W. B. Pratt.** 1985. Evidence that the 90-kDa phosphoprotein associated with the untransformed L-cell glucocorticoid receptor is a murine heat shock protein. J. Biol. Chem. **260**:12398–12401.
53. **Sato, S., N. Fujita, and T. Tsuruo.** 2000. Modulation of Akt kinase activity by binding to Hsp90. Proc. Natl. Acad. Sci. USA **97**:10832–10837.
54. **Stancato, L. F., A. M. Silverstein, J. K. Owens-Grillo, Y. H. Chow, R. Jove, and W. B. Pratt.** 1997. The hsp90-binding antibiotic geldanamycin decreases Raf levels and epidermal growth factor signaling without disrupting formation of signaling complexes or reducing the specific enzymatic activity of Raf kinase. J. Biol. Chem. **272**:4013–4020.
55. **Stravopodis, D. J., L. H. Margaritis, and G. E. Voutsinas.** 2007. Drug-mediated targeted disruption of multiple protein activities through functional inhibition of the Hsp90 chaperone complex. Curr. Med. Chem. **14**: 3122–3138.
56. **Taguwa, S., T. Okamoto, T. Abe, Y. Mori, T. Suzuki, K. Moriishi, and Y. Matsuura.** 2008. Human butyrate-induced transcript 1 interacts with hepatitis C virus NS5A and regulates viral replication. J. Virol. **82**:2631–2641.
57. **Tellinghuisen, T. L., K. L. Foss, and J. Treadaway.** 2008. Regulation of hepatitis C virion production via phosphorylation of the NS5A protein. PLoS Pathog. **4**:e1000032.
58. **Tellinghuisen, T. L., J. Marcotrigiano, and C. M. Rice.** 2005. Structure of the zinc-binding domain of an essential component of the hepatitis C virus replicase. Nature **435**:374–379.
59. **Terasawa, K., M. Minami, and Y. Minami.** 2005. Constantly updated knowledge of Hsp90. J. Biochem. **137**:443–447.
60. **Tomei, L., C. Failla, E. Santolini, R. De Francesco, and N. La Monica.** 1993. NS3 is a serine protease required for processing of hepatitis C virus polyprotein. J. Virol. **67**:4017–4026.
61. **Tu, H., L. Gao, S. T. Shi, D. R. Taylor, T. Yang, A. K. Mircheff, Y. Wen, A. E. Gorbalenya, S. B. Hwang, and M. M. Lai.** 1999. Hepatitis C virus RNA polymerase and NS5A complex with a SNARE-like protein. Virology **263**: 30–41.
62. **Wakita, T., T. Pietschmann, T. Kato, T. Date, M. Miyamoto, Z. Zhao, K. Murthy, A. Habermann, H. G. Krausslich, M. Mizokami, R. Bartenschlager, and T. J. Liang.** 2005. Production of infectious hepatitis C virus in tissue culture from a cloned viral genome. Nat. Med. **11**:791–796.
63. **Wang, C., M. Gale, Jr., B. C. Keller, H. Huang, M. S. Brown, J. L. Goldstein, and J. Ye.** 2005. Identification of FBL2 as a geranylgeranylated cellular protein required for hepatitis C virus RNA replication. Mol. Cell **18**:425–434.
64. **Wasley, A., and M. J. Alter.** 2000. Epidemiology of hepatitis C: geographic differences and temporal trends. Semin. Liver Dis. **20**:1–16.
65. **Watashi, K., N. Ishii, M. Hijikata, D. Inoue, T. Murata, Y. Miyanari, and K. Shimotohno.** 2005. Cyclophilin B is a functional regulator of hepatitis C virus RNA polymerase. Mol. Cell **19**:111–122.
66. **Whitesell, L., and S. L. Lindquist.** 2005. HSP90 and the chaperoning of cancer. Nat. Rev. Cancer. **5**:761–772.
67. **Wochnik, G. M., J. C. Young, U. Schmidt, F. Holsboer, F. U. Hartl, and T. Rein.** 2004. Inhibition of GR-mediated transcription by p23 requires interaction with Hsp90. FEBS Lett. **560**:35–38.
68. **Wolk, B., B. Buchele, D. Moradpour, and C. M. Rice.** 2008. A dynamic view of hepatitis C virus replication complexes. J. Virol. **82**:10519–10531.
69. **Yang, G., D. C. Pevear, M. S. Collett, S. Chunduru, D. C. Young, C. Benetatos, and R. Jordan.** 2004. Newly synthesized hepatitis C virus replicon RNA is protected from nuclease activity by a protease-sensitive factor(s). J. Virol. **78**:10202–10205.
70. **Zhong, J., P. Gastaminza, G. Cheng, S. Kapadia, T. Kato, D. R. Burton, S. F. Wieland, S. L. Uprichard, T. Wakita, and F. V. Chisari.** 2005. Robust hepatitis C virus infection in vitro. Proc. Natl. Acad. Sci. USA **102**:9294–9299.

Downloaded from jvi.asm.org at Osaka University on September 23, 2009

Biological and immunological characteristics of hepatitis E virus-like particles based on the crystal structure

Tetsuo Yamashita[a,1], Yoshio Mori[a,1], Naoyuki Miyazaki[b,c], R. Holland Cheng[c], Masato Yoshimura[d], Hideaki Unno[e], Ryoichi Shima[a], Kohji Moriishi[a], Tomitake Tsukihara[b], Tian Cheng Li[f], Naokazu Takeda[f], Tatsuo Miyamura[f], and Yoshiharu Matsuura[a,2]

[a]Department of Molecular Virology, Research Institute for Microbial Diseases and [b]Department of Protein Crystallography, Research Institute for Protein Research, Osaka University, Osaka 565-0871, Japan; [c]Department of Molecular and Cellular Biology, University of California, Davis, CA 95616; [d]National Synchrotron Radiation Research Center, 101 Hsin-Ann Road, Hsinchu Science Park, Hsinchu 30076, Taiwan; [e]Department of Applied Chemistry, Faculty of Engineering, Nagasaki University, Nagasaki 852-8521, Japan; and [f]Department of Virology II, National Institute of Infectious Diseases, Tokyo 208-0011, Japan

Edited by Michael G. Rossmann, Purdue University, West Lafayette, IN, and approved June 8, 2009 (received for review April 3, 2009)

Hepatitis E virus (HEV) is a causative agent of acute hepatitis. The crystal structure of HEV-like particles (HEV-LP) consisting of capsid protein was determined at 3.5-Å resolution. The capsid protein exhibited a quite different folding at the protruding and middle domains from the members of the families of *Caliciviridae* and *Tombusviridae*, while the shell domain shared the common folding. Tyr-288 at the 5-fold axis plays key roles in the assembly of HEV-LP, and aromatic amino acid residues are well conserved among the structurally related viruses. Mutational analyses indicated that the protruding domain is involved in the binding to the cells susceptive to HEV infection and has some neutralization epitopes. These structural and biological findings are important for understanding the molecular mechanisms of assembly and entry of HEV and also provide clues in the development of preventive and prophylactic measures for hepatitis E.

capsid | HEV | VLP

Hepatitis E is an acute viral hepatitis caused by infection with hepatitis E virus (HEV) that is transmitted primarily by a fecal-oral route (1, 2). Numerous epidemic and sporadic cases have occurred in developing countries of Asia, the Middle East, and North Africa, where sanitary conditions are not well-maintained. Hepatitis E affects predominantly young adults, and HEV infection in pregnancy is one of the risk factors for severe disease and death (3). Recent epidemiological studies show that significant prevalence of HEV and anti-HEV antibody is found in humans and several animals worldwide, even in developed countries (4–8).

HEV is the sole member of the genus *Hepevirus* within the family *Hepeviridae* and has a 7.2-kb positive-sense RNA genome (9). Five major genotypes have been identified so far (2). The viruses in the genotypes 1 and 2 are maintained among only humans, while those in the genotypes 3 and 4 are found in pigs or wild animals (4–6). However, infections of human with genotypes 3 and 4 via zoonotic transmission or blood transfusion were reported in the developed countries, such as Japan and the United States (7, 8, 10), suggesting that hepatitis E caused by infection with genotypes 3 and 4 of HEV is an important emerging infectious disease. The viruses in the genotype 5 are of avian origin and are thought to be uninfectious to humans (11). The genomic RNA contains three ORFs (ORFs) encoding nonstructural proteins (ORF1), the viral capsid protein composed of 660 amino acids (ORF2) and a small phosphorylated protein of unidentified function (ORF3) (1, 9). The viral capsid protein induces neutralizing antibodies by its immunization (12–15) or during the course of infection (16, 17). A typical signal sequence at the N terminus and 3 potential *N*-glycosylation sites (Asn-X-Ser/Thr) are well-conserved in the capsid protein derived from all mammalian genotypes (18, 19), but the glycosylation status of this protein is still controversial and the biological significance of the modification in the viral life cycle remains unknown. Although propagation of HEV in the cell culture systems reported in earlier studies was not efficient (20–23), Tanaka et al. succeeded in the establishment of a persistent infection system of HEV genotype 3 in human hepatoma (PLC/PRF/5) and human carcinomic alveolar epithelial (A549) cell lines (24). However, sufficient amounts of viral particles cannot be obtained for studies of the structure, life cycle, and pathogenesis of HEV.

Electron microscopy of human stool specimens showed that HEV is a nonenveloped spherical particle with a diameter of approximately 320 Å (25). As an alternative to in vitro propagation of HEV, the baculovirus expression system opens the prospect of studying HEV capsid assembly, since HEV-like particles (HEV-LP) with protruding spikes on the surface can be formed in insect cells infected with a recombinant baculovirus expressing the capsid protein of a genotype 1 strain (26–28). Cryo-electron microscopic (cryoEM) analysis has revealed that HEV-LP is a $T = 1$ icosahedral particle composed of 60 copies of truncated products of ORF2 (27, 28). The HEV-LP appeared to be empty due to a lack of significant density containing RNA inside and was 270 Å in diameter (26–28), which is smaller than the diameter of the native virions. However, the HEV-LP retained the antigenicity and capsid formation of the native HEV particles.

The crystal structures of the recombinant or native $T = 3$ viral particles derived from structurally related mammalian and plant viruses, such as recombinant Norwalk virus (rNV; PDB accession code 1IHM) (29), San Miguel sea lion virus (SMSV; PDB accession code 2GH8) (30), the members of the family *Caliciviridae*, and Carnation mottle virus (CARMV; PDB accession code 1OPO) (31), a member of the family *Tombusviridae*, have

Author contributions: T.Y., Y. Mori, T.T., T.C.L., N.T., T.M., and Y. Matsuura designed research; T.Y., Y. Mori, R.S., K.M., T.C.L., N.T., and Y. Matsuura performed research; T.Y., Y. Mori, N.M., R.H.C., M.Y., and H.U. analyzed data; and T.Y., Y. Mori, and Y. Matsuura wrote the paper.

The authors declare no conflict of interest.

This article is a PNAS Direct Submission.

Data deposition: The atomic coordinates have been deposited in the Protein Data Bank, www.pdb.org (PDB ID code 2ZTN).

[1]T.Y. and Y. Mori contributed equally to this work.

[2]To whom correspondence should be addressed at: Department of Molecular Virology, Research Institute for Microbial Diseases, Osaka University, 3-1 Yamadaoka, Suita-shi, Osaka 565-0871, Japan. E-mail: matsuura@biken.osaka-u.ac.jp.

This article contains supporting information online at www.pnas.org/cgi/content/full/0903699106/DCSupplemental.